



UNIVERSIDAD DE INVESTIGACIÓN DE TECNOLOGÍA EXPERIMENTAL YACHAY

Escuela de Ciencias Biológicas e Ingeniería

TÍTULO: Detection of Brain Pathologies by Machine Learning Using EEG Signals (1D) and EEG Surface Images (3D): Comparative Analysis.

Trabajo de integración curricular presentado como requisito para
la obtención del título de **Ingeniero Biomédico**

Autor:

Daniel Alfredo Amaguaña Marmol

Tutor:

PhD. Almeida Galárraga Diego Alfonso

Urcuquí, septiembre 2022

Autoría

Yo, **Daniel Alfredo Amaguaña Marmol**, con cédula de identidad 1724972714, declaro que las ideas, juicios, valoraciones, interpretaciones, consultas bibliográficas, definiciones y conceptualizaciones expuestas en el presente trabajo; así cómo, los procedimientos y herramientas utilizadas en la investigación, son de absoluta responsabilidad de el/la autora (a) del trabajo de integración curricular. Así mismo, me acojo a los reglamentos internos de la Universidad de Investigación de Tecnología Experimental Yachay.

Urququí, noviembre 2022.

Daniel Alfredo Amaguaña Marmol

CI: 1724972714

Autorización de Publicación

Yo, **Daniel Alfredo Amaguaña Marmol** con cédula de identidad 1724972714, cedo a la Universidad de Investigación de Tecnología Experimental Yachay, los derechos de publicación de la presente obra, sin que deba haber un reconocimiento económico por este concepto. Declaro además que el texto del presente trabajo de titulación no podrá ser cedido a ninguna empresa editorial para su publicación u otros fines, sin contar previamente con la autorización escrita de la Universidad.

Asimismo, autorizo a la Universidad que realice la digitalización y publicación de este trabajo de integración curricular en el repositorio virtual, de conformidad a lo dispuesto en el Art. 144 de la Ley Orgánica de Educación Superior

Urququí, noviembre 2022.

Daniel Alfredo Amaguaña Marmol

CI: 1724972714

Dedication

This thesis is dedicated to my entire family. Mainly to my parents, who supported me unconditionally in every possible way. Thank you for always trusting me and making me the person I am today, instilling sound principles and values, and teaching me perseverance and discipline. All this with sincere love and without asking for anything in return. They help me achieve the balance that allows me to give my full potential. I will never stop being grateful for this.

I also dedicate this work to my Ph.D. thesis tutor Diego Almeida who was a fundamental axis in the development of this project and who, more than a professor, has become a friend and future colleague. In the same way, I give a special dedication to God for giving me inspiration and strength to complete this work and, with this, fulfill one of my most desired desires, to finish my university career.

Daniel Amaguaña Marmol

Acknowledgments

This work was possible thanks to the unconditional support of my family. They were always by my side, motivating me to continue despite adversity, and have believed in me entirely. Thanks also to my friends who accompanied me during these university years and made my stay at Yachay Tech University unforgettable. In the same way, I want to express my deep gratitude to all the teachers who have contributed to my personal and professional training. Especially to my thesis advisor, Ph.D. Diego Almeida for the time and effort he gave while developing this work. His helpful hints and tips were of great help to me during the completion of this project. To my fellow directors from EMBS and Biomedical Engineering Club to the sick of 38, and Naomi N. They have made this path a unique experience. Finally, thank the platforms of free access to information that make knowledge available to everyone.

Infinite thanks to all of you and, of course, to God, for putting you on my path!!

Daniel Amaguaña Marmol

Resumen

El electroencefalograma es el método no invasivo utilizado en la actualidad para detectar anomalías en el funcionamiento del cerebro. Sin embargo, se requiere un gran conocimiento por parte de los médicos encargados de la detección de patologías. Con el fin de facilitar el reconocimiento de enfermedades y agilizar los procesos de investigación en torno al cerebro, se propone el siguiente proyecto, que consta de dos etapas. En el primero, se buscarán conjuntos de datos de señales electroencefalográficas (EEG) en una dimensión (1D) en repositorios de investigación de ciencias médicas como PhysioNet, Zenodo and RepOD. Luego utilizará inteligencia artificial para crear una red neuronal para conocer el porcentaje de éxito en la detección de patologías a través de señales EEG en una dimensión (1D). Una vez obtenidos estos resultados en la segunda etapa, las señales EEG se someterán a un procesamiento de señales con herramientas matemáticas y computacionales para transformarlas en señales de superficie sEEG en tres dimensiones (3D). Luego, las señales serán evaluadas a través de otra red neuronal para determinar el grado de éxito en las detecciones patológicas. Finally, a statistical comparison was made between works previously carried out in 1D and 3D dimensions.

Palabras clave: Electroencefalograma, redes neuronales, esquizofrenia, epilepsia, imágenes sEEG
MATLAB-EEGLAB, Python.

Abstract

The electroencephalogram (EEG) is the non-invasive method used today to detect abnormalities in the brain's functioning. However, a great deal of knowledge is required from the doctors in charge of the arrest of pathologies. In order to facilitate the recognition of diseases and streamline research processes around the brain, it is proposed the following project, which consists of two stages. In first, data sets of electroencephalographic (EEG) in one-dimension(1D) signals will be searched in medical science research repositories such as PhysioNet, Zenodo, and, RepOD. It will then use artificial intelligence to create a neural network to know the percentage of success in detecting pathologies through EEG signals in one dimension (1D). Once these results are obtained in the second stage, the EEG signals will be subjected to signal processing with mathematical and computational tools to transform them into surface signals sEEG signals in three dimensions (3D). Then, signals will be evaluated through another neural network to determine the degree of success in pathological detections. Finally, a statistical comparison will be made between the EEG signal (1D) and the EEG surface signals (3D).

Keywords: Electroencephalogram, neural networks, schizophrenia, epilepsy, sEEG images, MATLAB-EEGLAB, Python.

Contents

Chapter 1: Introduction	1
1.1. Problem Statement	1
1.2. Thesis Overview.....	2
Chapter 2: Objectives and Hypothesis	3
2.1. Objectives.....	3
2.1.1. General Objective.....	3
2.1.2. Specific Objectives.....	3
2.2 Hypothesis.....	4
Chapter 3: State of the Art	5
3.1 Nervus system physiology.....	5
3.1.1 Central nervous system	6
3.2 Electroencephalography	7
3.3 Schizophrenia.....	9
3.4 Epilepsy.....	10
3.5 Computer Fundamentals.....	11
3.5.1 Neural Networks (NN).....	11
3.5.2 Convolutional Models	12
Chapter 4: Methodology	13
4.1 Preprocessing data.....	13
4.1.2 Collect EEG data/datasets	15
4.1.2.1 Schizophrenia.....	15
4.1.2.2 Epilepsy.....	15
4.1.3 Import events channel and location	16
4.1.4 Filter data	17

4.1.5 Delete unwanted channels	19
4.1.6 Independent components analysis applied to EEG time series	20
4.2 Transformation of signals (1D) to 3D spectrograms.....	22
4.3 Data classification	23
4.4 Construction of neural network models.....	25
4.4.1 1D-CNN Model	25
4.4.2 3D-CNN Model.....	26
4.4.3 Cross-Validation	28
4.4.4 L2-Regularization.....	29
Chapter 5: Results	30
5.1 Signal preprocessing	30
5.2 Neural network models	31
5.2.1 Plots of Learning	31
5.2.2 Evaluation metrics.....	33
Chapter 6: Discussion	35
6.1 Data preprocessing analysis	35
6.2 Comparative analysis with other studies	36
Chapter 7: Conclusion.....	39
Bibliography	41
List of abbreviations	48

List of Tables

Table 1.	The functional role and position of the different areas of the cerebral cortex	7
Table 2.	Characteristics of brain EEG signals.	9
Table 3.	Detail of the 1D and 3D databases	24
Table 4.	Results metrics for model performance evaluation	34
Table 5.	Summary of recent models to diagnose schizophrenia using the Olejarczyk schizophrenia dataset.....	36
Table 6.	Summary of similar 3D schizophrenia prediction models.	37
Table 7.	Summary of recent models to diagnose epilepsy with signs.	38
Table 8.	Summary of recent models to diagnose epilepsy using imagen	38

List of Figures

Figure 1.	Diagram of the generalized nervous system and its parts. On the left is the central nervous system with the attributions of the sympathetic system, and on the right is the peripheral nervous system with the characteristics of the parasympathetic model. Own elaboration based on [9].	6
Figure 2.	Section a) contains the international standardized system for placing electrodes for recording 10-20 electron neurological signals. In section b) we can observe the main sections (lobes) in which the brain and the corresponding hemispheres are divided. Own elaboration based on [9, 12].....	8
Figure 3.	The neuronal synaptic communication cycle and its main parts transmit electrical signals. Calcium neurotransmitters are mainly present in synaptic neurotransmission. The curve of the action potential of the signal transmitted in voltage concerning time. Own elaboration from [30].	11
Figure 4.	Electroencephalographic data were preprocessing Own timeline elaboration based on [14].	14

Figure 5. In the upper part, two signals without preprocessing corresponding to patients S03 schizophrenic and epileptic ch03 are observed; the recording channels are displayed on the left of each image. The images at the bottom represent the same patients but with frequency and time compressed only for better visualization. Own elaboration extracted from MATLAB.....16

Figure 6. On the left, the channels of the schizophrenic patient S03 in 2D, system application 10-20. On the right side, the same 3D channel registration using polar coordinates is important for the spatial location of each channel. Own elaboration extracted from MATLAB.....17

Figure 7. Representation of high-pass filtering where the magnitude is represented in dB and the phase in degrees shows that the frequency is expressed in Hz. On the left side 0.5Hz high-pass filter, while on the left, there is a 50Hz low-pass filter.18

Figure 8. Comparison of line noise of the same channel C1, without left side filter vs. with right side filter. Own elaboration extracted from MATLAB.19

Figure 9. The spectrum of the signal, 100% of the data, is observed with the test frequency; it is helpful to analyze the atypical channels individually. Own elaboration extracted from MATLAB.....20

Figure 10. ICA decomposition and its components. On the left side are ocular components, muscular components, cardiac components, defective channel components, and brain components. On the right side are the typical spectra in terms of the power of each type of component. Own elaboration extracted from EEGLAB-MATLAB.....21

Figure 11. Process pathway of transformation of 1Da sEEGs. Data visualization, time-frequency analysis, and transformation to spectrograms. Own elaboration extracted from EEGLAB-MATLAB.....22

Figure 12. The first classification model consists of several layers with sub-blocks, each with Conv, activation function, max pooling, and Drop out. The number of input and output parameters and dimensions in each layer is detailed. Own elaboration.....25

Figure 13. The architecture of the 3D prediction model is based on image classification models. Own elaboration.27

Figure 14. Cross-validation diagram, equal segments [51].28

Figure 15. Preprocessing result. Data with noise and interference, data with the noise removal process, approximation of the amount of noise removed, final image spectrogram, and transformation of dimensions in data. Own elaboration.....31

Figure 16. 1D neural model learning graphs. In the upper part, the validation by learning is shown, as well as the loss of function due to Schizophrenia with signs. At the bottom are the learning and loss function graphs for epilepsy with signs. Own elaboration extracted from GOOGLE-COLAB.....	32
Figure 17. 3D neural model learning graphs. In the upper part, the validation by learning is shown, as well as the loss of function due to Schizophrenia with sEEGs. At the bottom are the learning and loss function graphs for epilepsy with sEEGs. Own elaboration extracted from GOOGLE-COLAB.....	32

List of Annex

Annex 1: EEG signal processing code and time segmentation.....	49
Annex 2: Transformation code from signals (1D) to surface images (3D).....	49
Annex 3: 3D convolutional model for images	50
Annex 4: 3D convolutional model for images	51

Chapter 1

Introduction

1.1. Problem Statement

According to the WHO, disorders of the nervous system (DNS) are the second leading cause of death in the world. That is 9 million deaths per year due to these brain pathologies. Disorders such as epilepsy, schizophrenia, migraine, dementia, meningitis, and Parkinson's are the most common. Low- and middle-income countries (LMICs) are the most affected. In these countries, treatment gaps exceed 75% in most LMICs and 50% in most middle-income countries. As a result of these differences, statistics show that around 80% of people with epilepsy and schizophrenia live in LMICs. Even disabilities associated with neurological conditions disproportionately affect those most affected: women, people living in poverty and rural or remote areas, and other vulnerable populations [1].

In Ecuador, brain pathologies are among the first 50 leading causes of death according to the Yearbook of vital statistics, births, and deaths, carried out by the National Institute of Statistics and Censuses (INEC) in 2014 [2]. Furthermore, indigenous populations, ethnic minorities, and Low-income children are at increased risk of disability associated with BP. In fact, in a study of untreated epilepsy in Ecuador. The cumulative annual incidence rate was 190 per 100,000, and the prevalence rate of active

epilepsy was 7 per 1,000, demonstrating a remission rate of 46%. One possible cause is that anti-seizure medications are not readily available [3].

The most effective ways to solve this problem or reduce the damage caused by neurological disorders worldwide are constant monitoring, early detection, and appropriate medication for each brain pathology [4].

1.2. Thesis Overview

This research is structured as follows: chapter 1 collects the problem and the general vision of the project approach. Chapter 2 sets out the general and specific objectives of the project. After that, they continue with chapter 3, which contains essential information for understanding brain pathologies, their monitoring, and detection. In addition, it explains the structure of the data in 1D and 3D. Also, the methods to process them as well as neural networks. Then chapter 4 focuses on the methodology, the preprocessing, and the processing of signals and images, respectively. In addition, the chapter talks about training artificial intelligence models with their different neural networks. Next, chapter 5 focuses on the presentation of the results of their training models and the discussion of these results, comparing them with previous work. Finally, chapter 6 reflects the conclusions reached based on the objectives and prospects.

Chapter 2

Objectives and Hypothesis

2.1. Objectives

2.1.1. General Objective

Perform two models and prediction of brain pathologies through the analysis of electroencephalographic (1D) EEG signals and sEEG (3D) images, using artificial intelligence and machine learning through two neural networks.

2.1.2. Specific Objectives

- To obtain a sufficiently robust dataset of electroencephalographic signals to train the brain pathology prediction model and with the optimal characteristics to process it in the Google Colab software with the python language program.
- Efficiently transform electroencephalographic signals (1D) into surface electroencephalographic images (3D) for subsequent analysis in artificial intelligence models without losing information.
- Create a prediction model with a short-term and extended memory recurrent neural network to analyze the signals (1D). On the other hand, make prediction models with a convolutional neural network (CNN) to analyze the sEEG images (3D). Obtain a data set of

electroencephalographic signals and images sufficiently robust to train the brain pathology prediction model and the optimal characteristics to process them.

- Perform a comparative analysis between the prediction results of brain pathologies obtained by the first model with signal analysis (1D) and the second with sEEG image models.
- Determine the best data type used for the optimal prediction of brain pathologies after having processed the data by each model. Also, compare the models of previous work in artificial intelligence related to the study of EEG signals and images.

2.2 Hypothesis

Brain pathologies can be predicted with high precision through machine learning tools using brain EEG signals (1D) and sEEG surface imaging (3D).

Chapter 3

State of the Art

3.1 Nervus system physiology

The nervous system is one of the most challenging systems of the body to understand due to it being a complex organization. It is the system in charge of receiving and processing all the information that comes from outside and inside the body to regulate the responses exerted by the other organs and systems; this response can be in collaboration with the endocrine system for the release of different hormones [5]. The cells in charge of carrying the information in the system are the neurons; They have a cell body and an axon with a synaptic area at its ends [6]. The signal that travels through the neurons is electrical and is caused by depolarization of the axonal membrane; this produces an axon potential that passes through an area of communication between neurons [7]. Neurons are differentiated by their function and organization in routes or networks that can be ascending or descending. In two ways, from the periphery (receptors) to the brain area involved in interpreting the type of signal OR from the cerebral cortex to the periphery [8].

The CNS comprises the spinal cord and the brain Figure 1. On the other hand, the peripheral nervous system comprises all the nerves that branch off from the spinal cord and extend to all parts of the body [7].

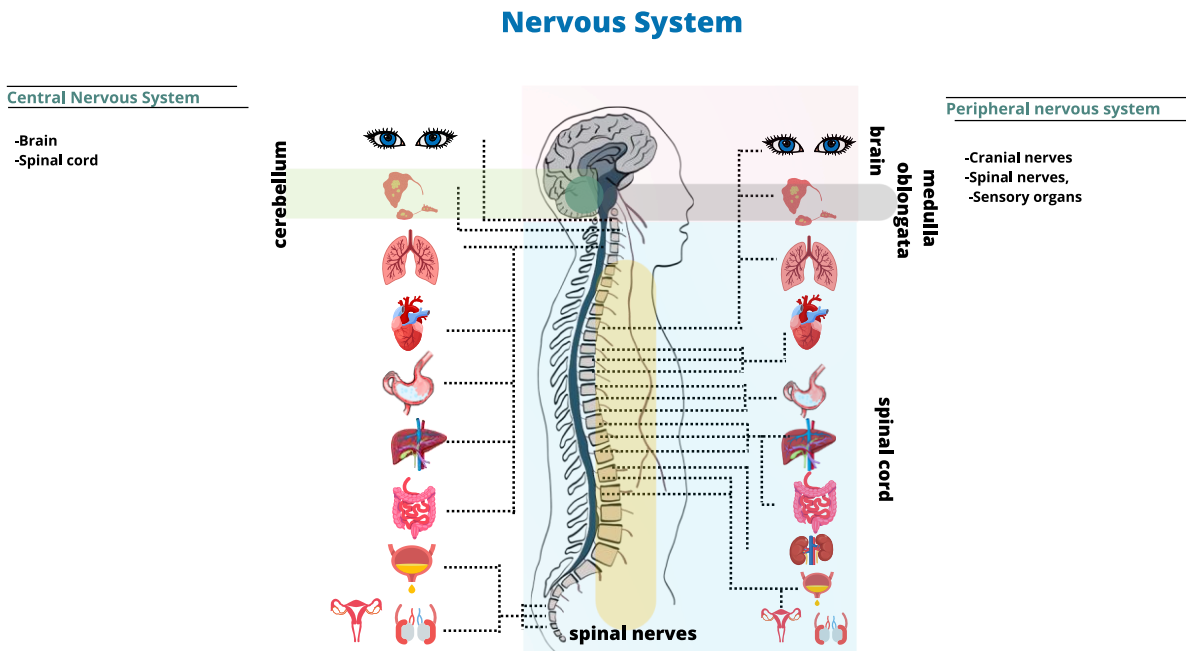


Figure 1. Diagram of the generalized nervous system and its parts. On the left is the central nervous system with the attributions of the sympathetic system, and on the right is the peripheral nervous system with the characteristics of the parasympathetic model. Own elaboration based on [9].

3.1.1 Central nervous system

The central nervous system has a bidirectional task that allows it to control most of the body's functions. Since it makes possible the transmission of signals-body, the CNS can be made up of two main parts that are: the cerebral cortex and the subcortical regions that are responsible for controlling vital functions such as reflexes, temperature regulation, breathing, heart rate as well as the ability to memorize and learn [8, 10]. Each lobe can be identified by the folds of each hemisphere (right and left) separated by four grooves. The central one, Rolando's groove, lateral, parieto-occipital, and occipital temporal [11]. The individualizations make up the surface, the lobes: frontal, parietal, occipital, temporal, and within the insular lobe shown in Table1

Table 1. The functional role and position of the different areas of the cerebral cortex

Cortex zones	Lobes				Functions
	Frontal	Parietal	Temporal	Occipital	
Primary or projection	4	1,2,3	41,42	17	Receive chemical or physical stimuli from the sense organs.
Secondary or association	6,8	5,7	21,22	18	Fulfill multimodal functions of importance
Tertiary or integration	9,10,11,45, 46	39,40	21	19	Integration functions that allow different groups of neurons to work in concert.

Own elaboration based on [12]

3.2 Electroencephalography

An electroencephalogram (EEG) is a biomedical signal meter that measures the electrical activity generated by the firing of neurons within the human brain over time [13]. EEG signals are measured using electrodes attached to the scalp, which are sensitive to changes in the postsynaptic potentials of neurons in the cerebral cortex. Electrodes are usually placed along the scalp following the 10-20 International System of Electrode Placement (Fig 2. a) developed by Dr. Herbert Jasper in the 1950s, allowing for standard measurements of various brain parts [14]. The EEG frequency range is classified into oscillatory neural patterns: delta (1–3 Hz), theta (4–7 Hz), alpha (7–12 Hz), Mu (8-13), beta (12–30 Hz), and gamma-band oscillations (>30 Hz) [15], more details are shown in Table 2.

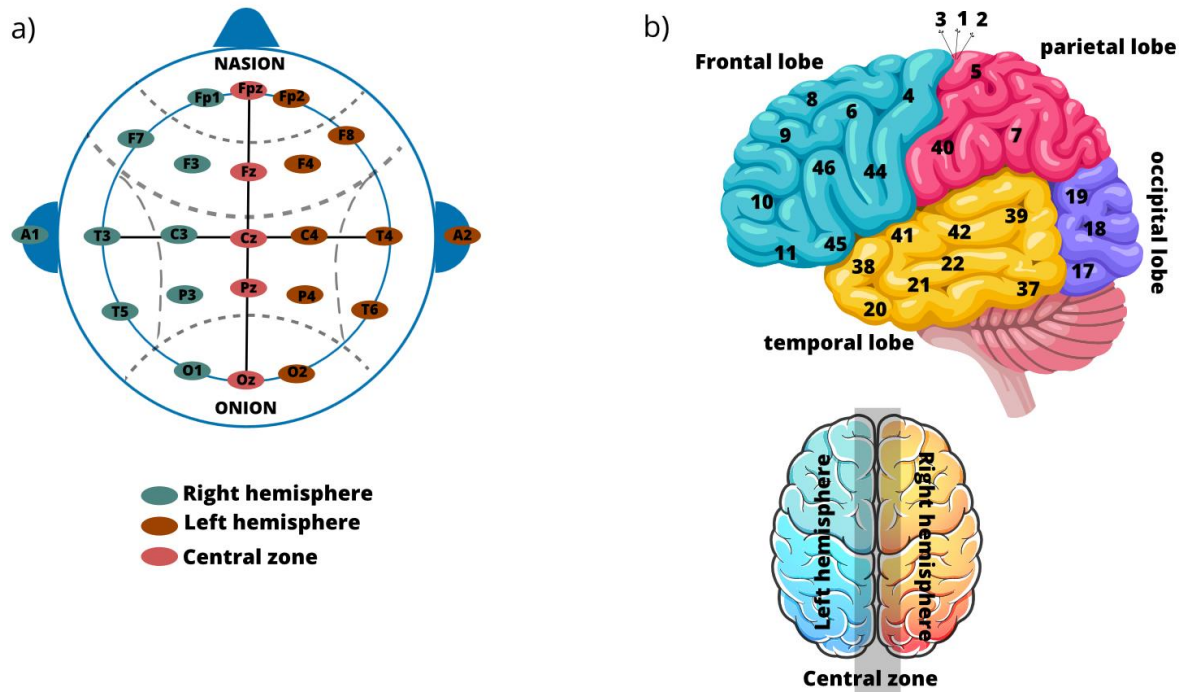








Figure 2. Section a) contains the international standardized system for placing electrodes for recording 10-20 electron neurological signals. In section b) we can observe the main sections (lobes) in which the brain and the corresponding hemispheres are divided. Own elaboration based on [9, 12]

The EEG is one of the easiest and cheapest functional neuroimaging tools [13]. The brain's electrical activities are recorded from the head surface with a high temporal resolution and an appropriate spatial resolution, which is influential in brain pathologies diagnosis [16]. Neurological conditions reflected in EEG help identify people with mental disorders from healthy controls. This is possible as brain behavior differs for both groups, as shown in Figure 2.

Table 2. Characteristics of brain EEG signals.

Type EEG waves	Frequency (Hz)	Localization Zone	Mental Activity	Shape
Delta	1-3	front area for adults, the rear area for children theta	Slow wave, deep sleep-in babies.	
Theta	4-7	median frontal line	drowsiness, meditation, unconscious.	
Alpha	7-12	right and left posterior regions	Relaxation and concentration.	
Mu	8-13	sensorimotor cortex	Well-functioning neurons.	
Beta	12-30	frontal area and sensorimotor cortex C3, C4	Vigilance, active concentration, thinking.	
Gamma	>30	somatosensory cortex	Somatosensory processing, short-term memory matching of recognized objects, tactile sensations.	

Own elaboration based on [17]

3.3 Schizophrenia

A *mental disorder* can be defined as a health condition that impairs a person's thinking, normal acting senses, or behavior and causes distress or difficulty in functioning[18]. The term mental disorder indicates a problem with the mind, not only in an abstract sense but also in a biological sense, that causes

modifications brain's processes to function correctly. Scientists study the chemical or structural changes that occur at the cellular level in the brain when someone has a mental disorder to develop better treatments or find a cure [19].

Schizophrenia is one of the most important mental disorders leading to disruption in brain growth [20, 21]. This disorder seriously damages thoughts, emotional expression, and also individuals' perception of reality [22]. The reason for Schizophrenia is not fully understood, though most research has demonstrated that the structural and functional abnormalities of the brain play a role in its creation [23]. According to the World Health Organization reports, nearly 21 million individuals worldwide suffer from such a brain disorder. The average age starting to get affected by this disorder is in youth age, in men at 18 years old and women at 25 years old, being more prevalent among males [24].

3.4 Epilepsy

Epilepsy presents with recurrent seizures (epileptic seizures) in patients [25]. These epileptic seizures are caused by sudden and abrupt changes in the brain's electrical function that produce physiological and motor alterations such as loss of consciousness, sudden movements, and temporary loss of breathing and memory; these usually occur in the cortex or outside the edge of the brain. Epilepsy can develop for various reasons, including abnormalities in the brain's network of interconnections [26, 27]. In addition, the devaluing of nerve signaling chemicals such as neurotransmitters can also change the above two reasons.

Generally, the area of the brain where abnormal electrical impulses occur during a seizure is the frontal lobe. Here are the neurons that usually generate impulses. Electrochemical that act on other neurons become unbalanced and act on glands and muscles to produce distorted thoughts, movements, feelings, and

irrational human actions. While epileptic seizures occur, the neurons' electrical activity increases up to 500 times (1-100 μV) of ordinary [28, 29], as shown in Fig. 3. Epilepsy can also be inherited due to genetic defects. Or also due to metabolic abnormalities, such as low glucose levels.

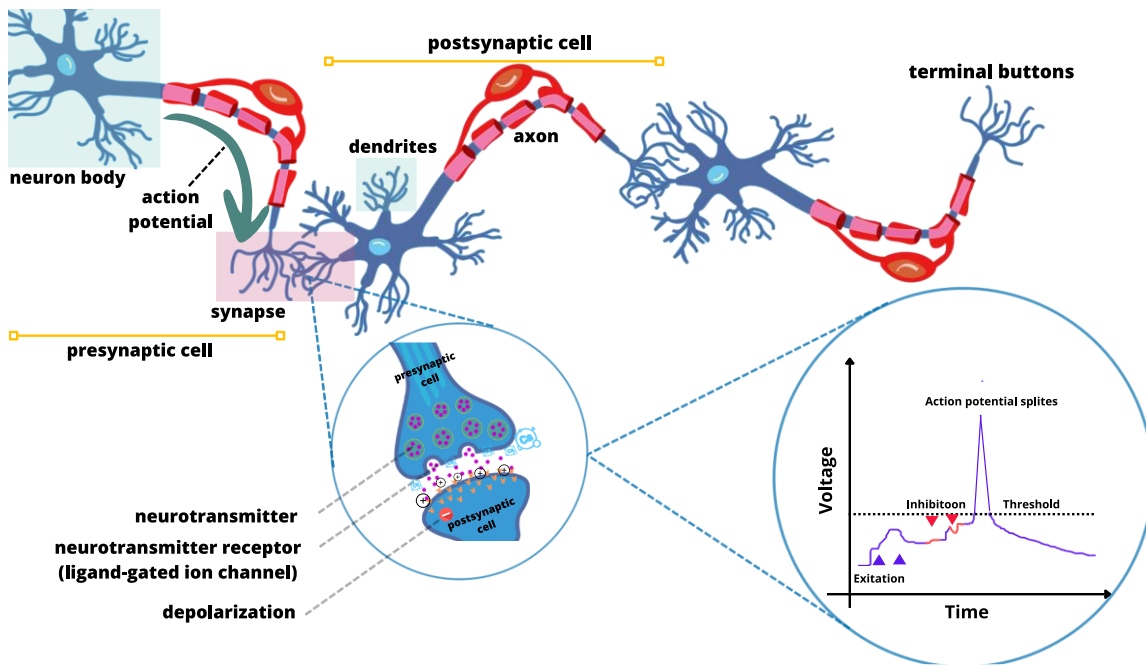


Figure 3. The neuronal synaptic communication cycle and its main parts transmit electrical signals. Calcium neurotransmitters are mainly present in synaptic neurotransmission. The curve of the action potential of the signal transmitted in voltage concerning time. Own elaboration from [30].

3.5 Computer Fundamentals

3.5.1 Neural Networks (NN)

Neural networks are computing tools that use deep and machine learning (ML) algorithms for data processing; their main task is to learn while automatically modifying themselves to perform complex tasks

that programming based on classical algorithms cannot perform [31, 32]. The working principle of the NN is to receive input values, then process them in a node called a neuron where the operation is executed, and, along with various activation functions, modeling optimally adjusted to a minor output error is performed [33]. There are several layers of neurons that form an NN; this depends on the optimization that is required [34]. This is how a new value is obtained at the end of the neuronal layers. Finally, this value is adjusted with internal statistical and mathematical processes such as gradient descent to have a small (almost zero) prediction error [35, 36].

3.5.2 Convolutional Models

Convolutional Neural Networks (CNNs) can fuse feature extraction and classification into one process that can be optimized to maximize the classification performance. This also eliminates the need for fixed and hand-crafted feature extraction. Conventional deep CNNs (i.e., 2D CNNs) were initially introduced to perform object recognition tasks for 2D signals, such as images, for various purposes [37–44]. In 1D-CNN models, signal time can be considered a spatial dimension, e.g., the height or width of a 2D image. The following hyper-parameters determine a 1D-CNN: 1) several hidden CNN and FC layers, 2) filter size, 3) subsampling factor, and 4) the choice of pooling and activation operators. It provides a low computational complexity since the only costly operation is a sequence of 1D convolutions that are linear weighted sums of two 1D arrays. The higher performance of CNN models in machine vision has led them to be used in time series processing, such as medical signals, leading to successful results [45, 46]

Chapter 4

Methodology

This project was developed in phases from which important stages were derived. At first, the construction of the data set (1D) obtained from different platforms of free use of EEG signal data destined for research was carried out. The dataset underwent preprocessing, which will be discussed later. This preprocessing is typical in the field of treatment and extraction of features in signals. Subsequently, the transformation of signals (1D) to surface images (3D), also called EEG spectrograms, were performed.

Once the data packages distributed by epilepsy and schizophrenia pathologies were obtained, the neural network models were built to compare the data. In this stage, it was necessary to develop specific automation and error control processes and optimize data processing and hyperparameter control. Next, the results of each neural network and its respective data sets were obtained, and known formulas were applied to find the measurement parameters of precision, sensitivity, and sensitivity. Finally, a comparative analysis was carried out between similar works carried out previously and the present study.

4.1 Preprocessing data

One of the fundamental and most important stages in predicting neuronal diseases is the stage before data classification. That is, the preprocessing of EEG data. It is important to preprocess the data as it comes out raw from a continuous recording device such as electroencephalographs or brain recording devices. However, it is required to extract the characteristics of these signals. Characteristics include Brain

oscillations, brain source activations, comparing brain data in different conditions, and valuating reliable (different potential) changes in external stimuli. An important tool used in the present work was the MATLAB software's EEGLAB extension, which allowed the preprocessed data corrector. To do this, several transformations are carried out in stages, which are detailed in Fig 4. In addition, the following sections will detail the most important stages of the preprocessing pipeline.

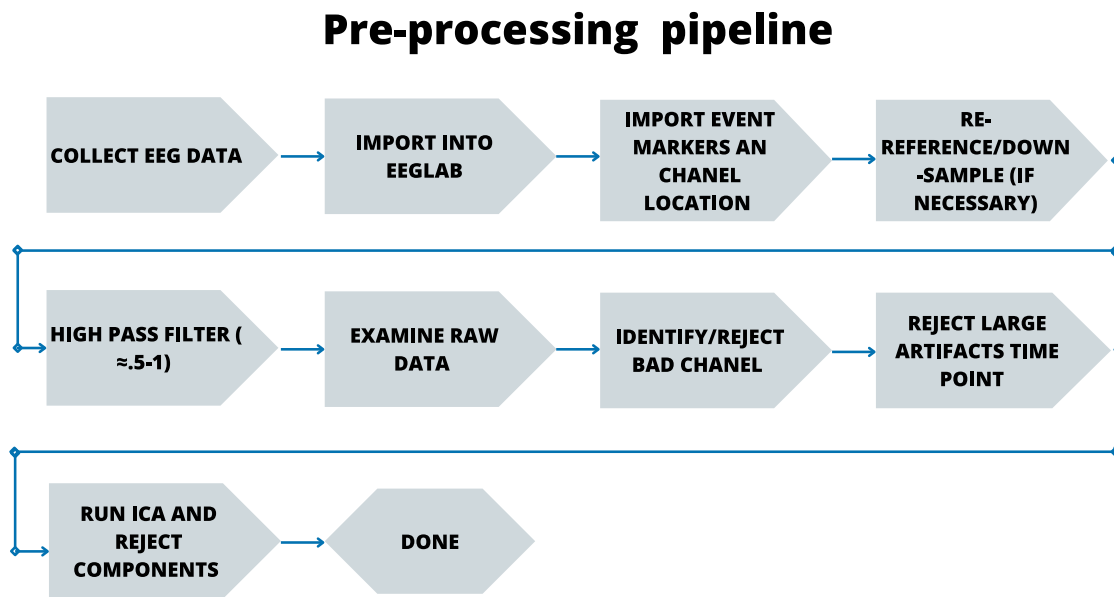


Figure 4. Electroencephalographic data were preprocessing Own timeline elaboration based on [14].

4.1.2 Collect EEG data/datasets

The data was acquired from open-access platforms for research purposes. The data set is about recordings of patients presenting with epileptic and schizophrenic seizures. As well as patients in a normal state without pathological events. For each pathology, times, frequency, channels, noise, and specific exceptions detailed in the following sections will be obtained.

4.1.2.1 Schizophrenia

Regarding schizophrenia data, data from the university was obtained [47], which consists of signals from encephalographic records of 14 healthy patients aged between 27-28 years. It also has records of 14 patients with schizophrenia at the same age as the healthy patients. The sampling of the signals counts for 15 minutes for each patient with their eyes closed to avoid noise from blinking and distractions. The data collection process was carried out with the 10-20 standard at a sampling frequency of 250 Hz. The electrodes used are detailed below[47, 48].

4.1.2.2 Epilepsy

This dataset was obtained for epilepsy screening from Children's Hospital Boston (CHB), and the Massachusetts Institute of Technology (MIT) created and contributed this database to PhysioNet consisted [49]. It is built with the registry of epileptic and healthy cases grouped into 23 cases, collected from 22 subjects (5 men, from 3 to 22 years of age, and 17 women, from 1.5 to 19 years of age). Each box (chb01, chb02, etc.) contains between 9 and 42 continuous .edf files at intervals of approximately 10 seconds with a sampling frequency of 248 Hz. Patient data is protected by international regulations [49, 50].

4.1.3 Import events channel and location

With the import of events and the location of the channels, we want to have the main idea of how the Figure X data sets are structured. Characteristics include the number of channels, amplitude, capture frequency, and abnormal events. Once the scheme of the events has been made, we proceed to work with the location of the channels. To do this, EEGLAB has an automatic channel characterization where labels are made for the channels associated with the recording samples so that if the channel is not yet available, it will be assigned or by default. The closest location is found with polar coordinates for both angles and radio. A global representation of 2D and 3D channels can be made in Fig 5.

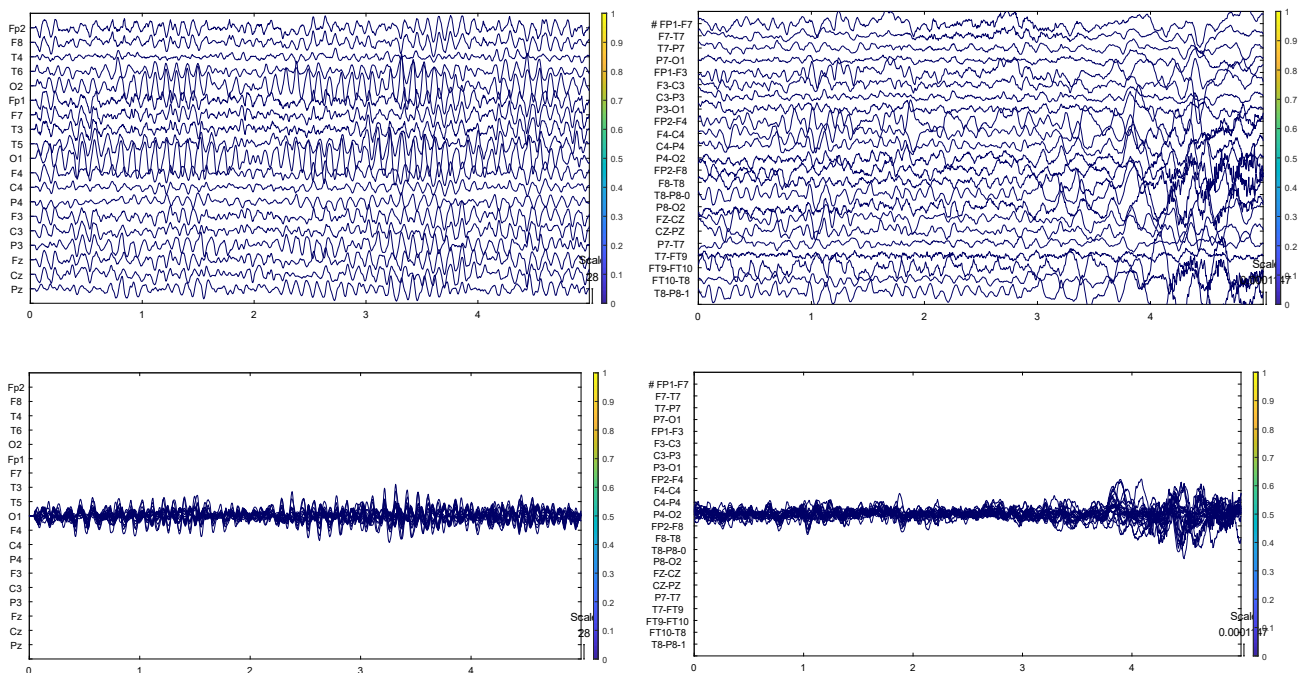


Figure 5. In the upper part, two signals without preprocessing corresponding to patients S03 schizophrenic and epileptic ch03 are observed; the recording channels are displayed on the left of each image. The images at the bottom represent the same patients but with frequency and time compressed only for better visualization. Own elaboration extracted from MATLAB.

Once obtained, they can appear in different dimensions. For example, you can optimize the center of the head, rotate the main axes along X0 +, select the given channels (autonomous, cardiac respiration), and optimize the electrodes' positions.

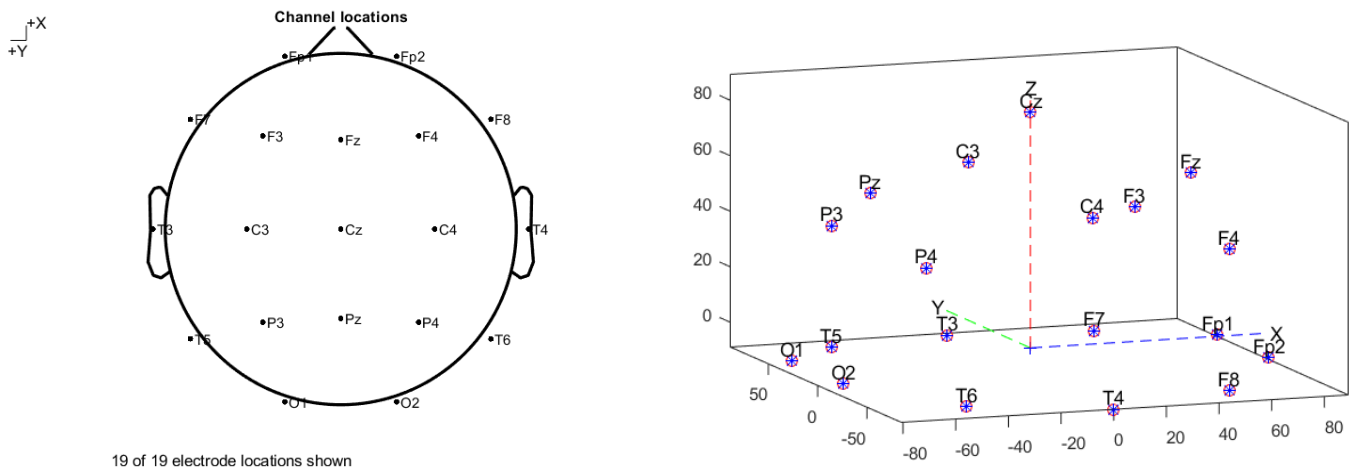


Figure 6. On the left, the channels of the schizophrenic patient S03 in 2D, system application 10-20. On the right side, the same 3D channel registration using polar coordinates is important for the spatial location of each channel. Own elaboration extracted from MATLAB.

4.1.4 Filter data

When the data has already been imported, the permanence of the channels is located and re-referenced (re-reference was not necessary for the present work). The filtering continues, and for this first, the blank shift of the signal is removed to avoid creating artifacts at the beginning and end of the movement; the filter used for this stage was a 0.5 Hz high pass limit filter. That is, anything below the mentioned frequency will be removed. This filter is taken because Independent Component Analysis (ICA) is

maintained to remove artifacts, and ICA is very sensitive to the lowest frequency shift. It is essential to mention that in case there are breathing channels, muscle contractions, or heart contractions, it is better not to filter them to keep the information intact.

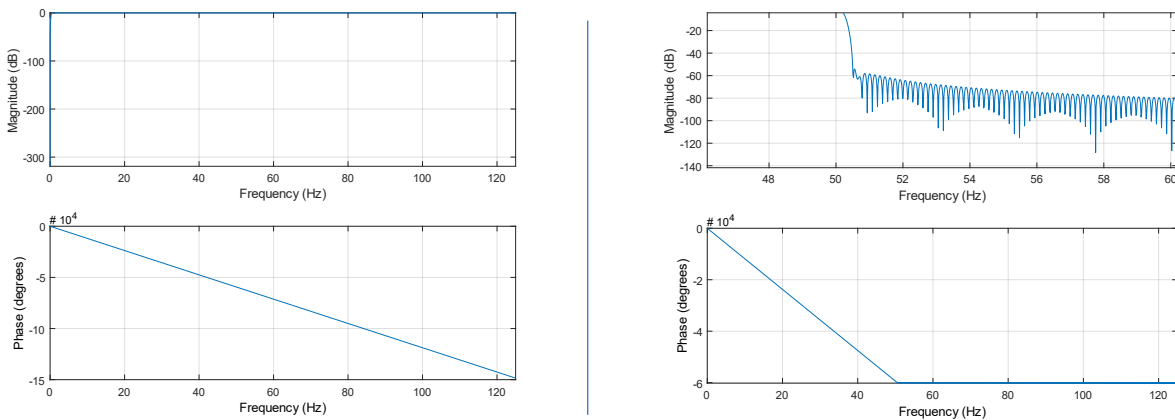


Figure 7. Representation of high-pass filtering where the magnitude is represented in dB and the phase in degrees shows that the frequency is expressed in Hz. On the left side 0.5Hz high-pass filter, while on the right, there is a 50Hz low-pass filter.

The frequency response, magnitude, and phase shift for the 0.5 Hz high pass filter are shown in Fig. 7. On the left side, while on the right side, we have what the response would look like to a low pass filter with 50 Filter rate Hz. Phase shift was reduced, and concerns about linearity were avoided because the direction in which the filter is applied is bidirectional. Clean line filtering was applied; this plugin works by trying to find the sinusoid that corresponds to the line noise and then subtracting that sinusoid; we can measure the window (4 seconds) and the frequency in both limits you want to delete. In this case, it was between [60;10].

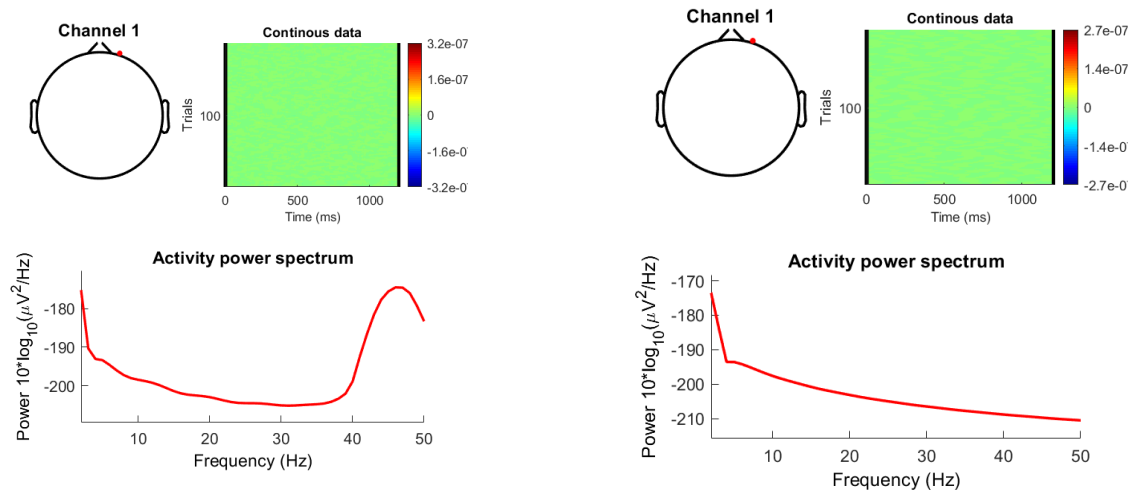


Figure 8. Comparison of line noise of the same channel C1, without left side filter vs. with right side filter. Own elaboration extracted from MATLAB.

Figure 8 shows the response to the method mentioned above. On the left side, a signal with noise exists throughout the path and specific line noise. However, the right side corresponds to the application of the clean line filter plus a 0.5 Hz high pass filter.

4.1.5 Delete unwanted channels

This section identifies and removes faulty channels from the EEG recording. In the manifestations, some channels have a frequency spectrum very far from average or do not present data; it is essential to identify this data and mark and eliminate them. In this case, they were: EXG5-ECG6-EXG7-EXG8. Although the temporary channels T3.T4.T5.T6 contain frequency noise due to their naturalness, they were not eliminated since important information on events could be lost. It is possible to visualize the elimination and the result that it implies in the complete signal on a scale from 0 to 1 μV Fig 9.

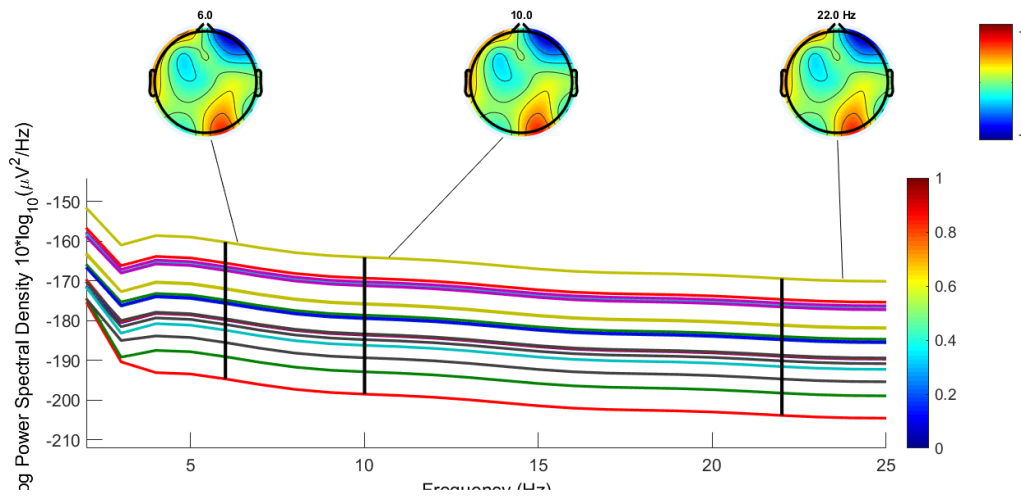


Figure 9. The spectrum of the signal, 100% of the data, is observed with the test frequency; it is helpful to analyze the atypical channels individually. Own elaboration extracted from MATLAB.

4.1.6 Independent components analysis applied to EEG time series

ICA is an independent component analysis in signal preprocessing to separate linearly mixed independent sources in several sensors. The principle that ICA has is to recover an original version of the recording where the data recorded in different channels are X , and ICA finds the W and U . Which are the mixing matrix and the activities of the source, respectively, Form 1.

$$(1) \quad X = WU$$

where, X = data channels x in time,
 U = ICA source activity
 W = ICA unmixing matrix

Independent analysis features for EEG that can be observed are artifacts, stimulus-triggered activity, response-triggered activity, non-phase-locked activity, event-modulated oscillatory activity, overlay maps, and spectra. And you can visualize a topography of the course of time-related brain

components, such as frontoparietal theta, central theta, and frontal midline theta. On the other hand, the occipital Alpha components are also present. In Figure 10, we can visualize the result of ICA, where we find components of various types, such as ocular, muscular and cardiac components, if applicable (in this case, it does not). This is how channel number 3 is presented, which presents a typical blinking eye movement with a curve with a 1/f spectrum and the activity of the component. Additionally, records of muscular movements are presented, as in channel 10, with a range with more power than the previous one. Channels with wrong signals can also be found where the target of the recording C2 and C13 is not located with pressure.

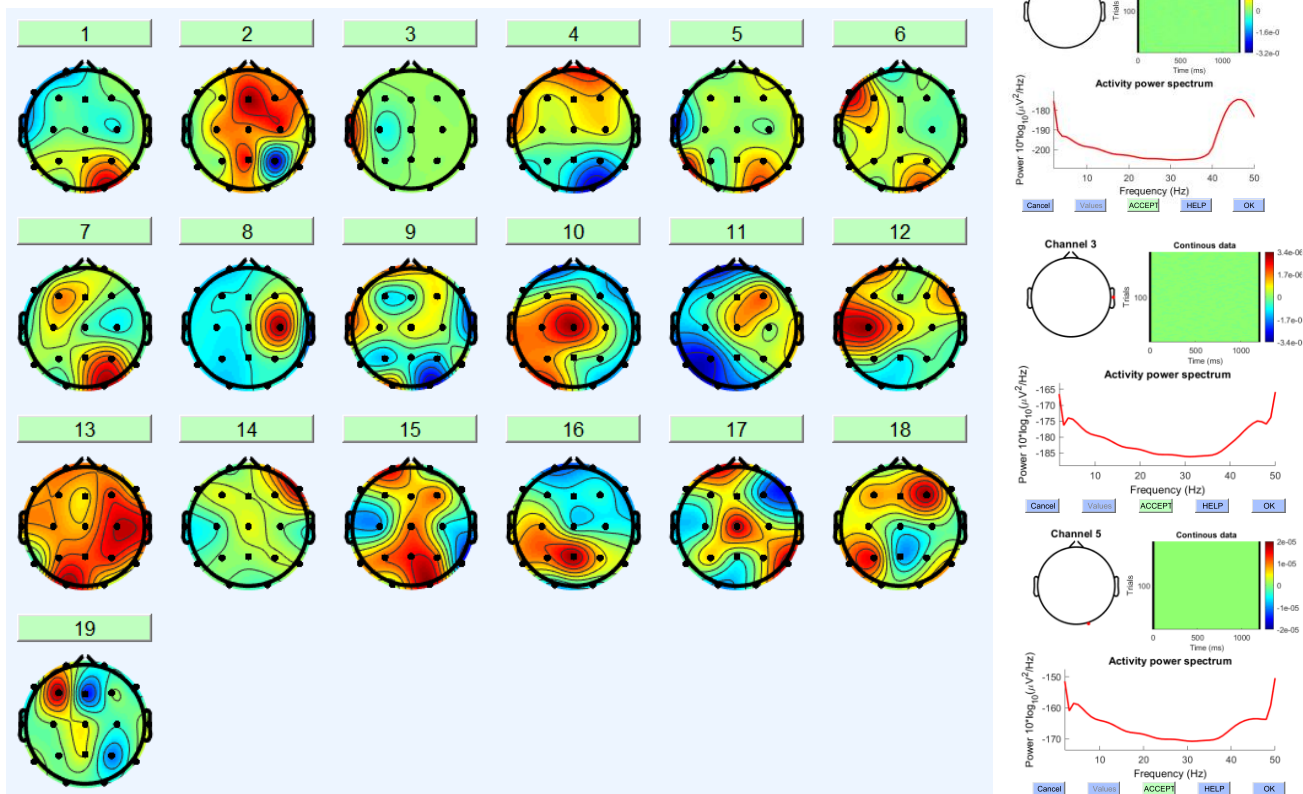


Figure 10. ICA decomposition and its components. On the left side are ocular components, muscular components, cardiac components, defective channel components, and brain components. On the right side are the typical spectra in terms of the power of each type of component. Own elaboration extracted from EEGLAB-MATLAB.

4.2 Transformation of signals (1D) to 3D spectrograms.

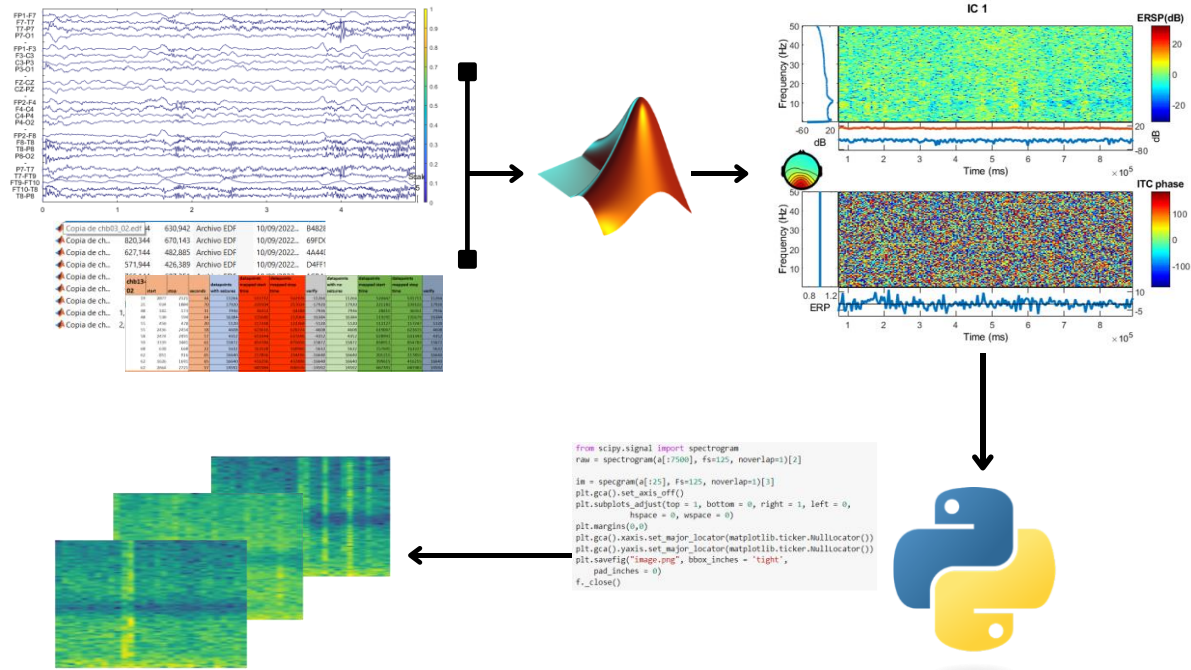


Figure 11. Process pathway of transformation of 1Da sEEGs. Data visualization, time-frequency analysis, and transformation to spectrograms. Own elaboration extracted from EEGLAB-MATLAB.

When we speak of an EEG in spectral form (spectrogram), we speak of an image that represents the composition of a signal in several dimensions, in this case, time, frequency, and energy. This way, the variation of the signal's frequency spectrum and the energy can be represented as a function of time. Thus, we can say that time is represented on the x-axis as the sequence of Fourier transforms, on the y-axis the frequency in Hz and determined as $\frac{1}{2}$ of the spectrum, and finally, the representation of energy in dB as the modulus of the amplitude of the Fourier transform, where dark colors represent the highest energy and lighter tones the lowest energy. To carry out this transformation, two tools were obtained: MATLAB with

its EEGLAB interface and its frequency, energy, and time graph to record and corroborate the expected energy levels in each surface image.

On the other hand, the block transformation of the set of signals to images was automated with Python algorithms. Figure 11 details the transformation process where the preprocessed data is first illustrated with the different filters, channel elimination, and ICA in formats .svc and .edf (2d). Second, a review of the time-frequency components of the data was carried out to assess the viability of the data to be used in subsequent stages, for which MATLAB-EEGLAB graphing tools were obtained. Thirdly, a transformation of signals to surface images was carried out through Python algorithms with libraries for classic data plots and matrix products such as Matplotlib, pyedflib, and NumPy.

In addition, the function "spect gram (a [:25], Fs=125, noverlap=1" defines associated parameters. Finally, a data set was made with all the final spectrograms obtained from this process. This was done for data without pathology of epilepsy and schizophrenia and for pathological data with events of both pathologies.

4.3 Data classification

Once the data was obtained and its respective transformation, they were classified as shown in Table 3. Where it is separated by pathology, then by the type of data, taking into account characteristics such as capture frequency, time of duration, number, and several patients. For data classification, it is necessary to separate each pathology into training and validation sets. Thus, it was distributed with a percentage of 80% training and 20% validation for the total data. In addition, 20 data units were separated for each neuronal disorder to observe the result when never-before-seen data was entered.

In the set of spectrograms, manual filtering was carried out, where 96 data were manually eliminated since the results of the pixels were too far from ordinary. In addition, the classified data is deleted randomly and taken into account that they comply with an equitable distribution to avoid overfitting the neural network.

Table 3. Detail of the 1D and 3D databases

Pathology	Data Type	Recording type	Sampling frequency (Hz)	Times	No. of patients	Reference
Epilepsy	Sings 1D	SCALP EEG	256	844	22	PhysioNet CHB-MIT
		SCALP EEG	256	74 min	79 Neonatal	Zenodo
	Images 3D	Spectrogram sEEG	256	5-second intervals. 2800 images	22 and 79 Neonatal	Made with Python, MATLAB
Schizophrenia	Sings 1D	SCALP EEG	250	250	14 with SZD and 14 healthy	RepOD IBIB_PAN
	Images 3D	Spectrogram sEEG	250	5-second intervals. 3000 images	14 with SZD and 14 healthy	Made with Python, MATLAB

Own elaboration

4.4 Construction of neural network models

4.4.1 1D-CNN Model

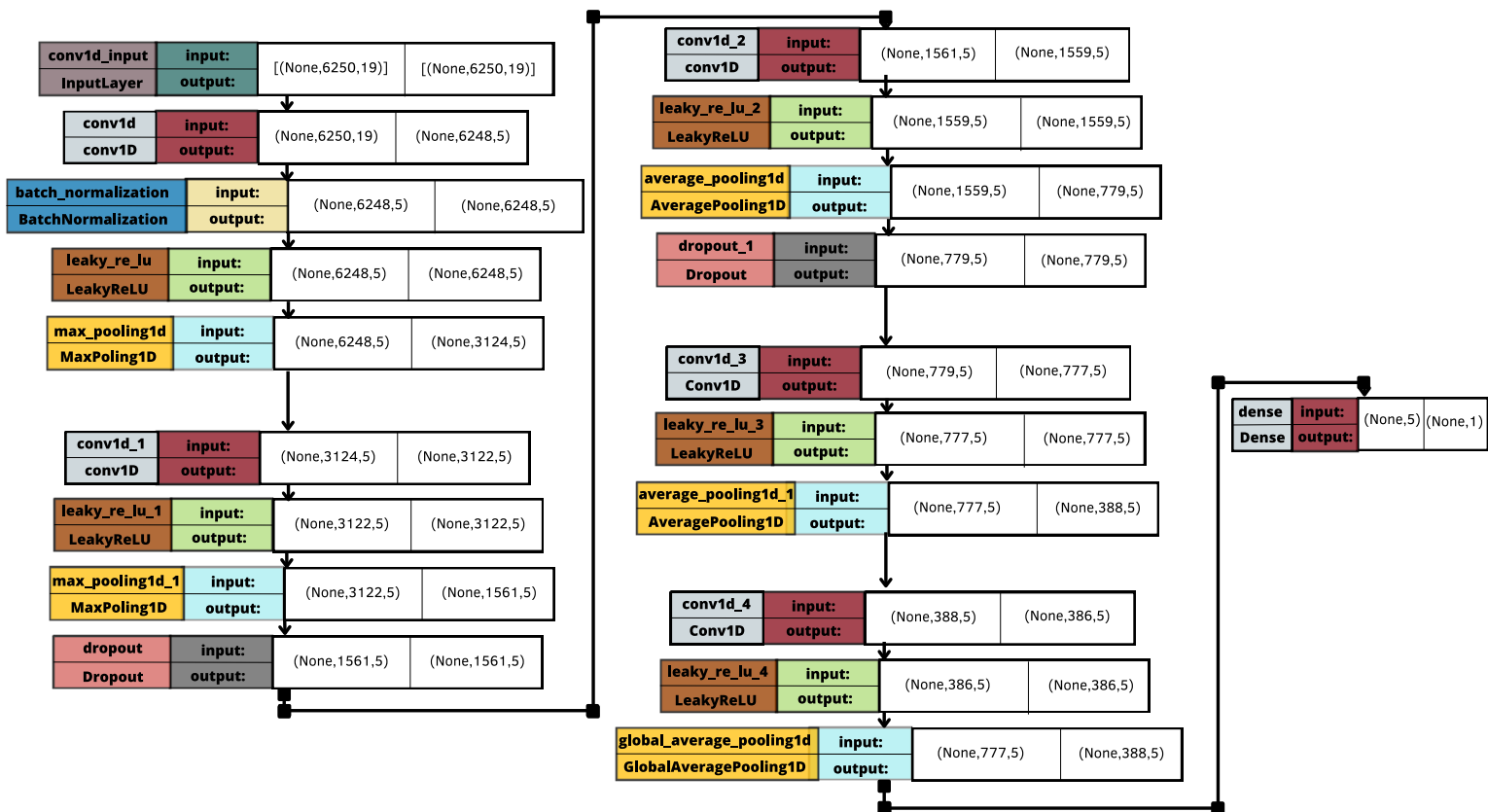


Figure 12. The first classification model consists of several layers with sub-blocks, each with Conv, activation function, max pooling, and Drop out. The number of input and output parameters and dimensions in each layer is detailed. Own elaboration.

The architecture of the 1D-CNN model for time-space contains regulators in each layer to optimize the process Fig 12. First, a 1-D convolutional layer with input from the temporal-spatial layer is added to produce an output tensor. Then, in the same block, batch normalization is applied to keep the means close

to zero and the standard deviation close to 1. Next, a LeakyReLU is added to have a small gradient when the unit is inactive. Finally, a Maxpooling layer is implemented to reduce the representation sample considering the maximum window value.

For the second layer, the first layer model is replicated but with the difference that it is implemented an (average-polling) to reduce the representation sample by calculating the average of the characteristics. At this stage, a (Dropout = 0.5) is also implemented. To eliminate (Overfitting). In this way, half of the neurons in training are left, resting randomly to speed up the learning process.

In the following layers, the model of the second layer is replicated up to layer 5 of convolution, maintaining the Average Poling and Dropout until the penultimate layer obtains a good enough trainability so that they can recognize data with schizophrenia. In layer 5, Global Polling is also implemented, which has the same principle as Average Pooling, except that the pool size is the size of the entire block input. That is, compute an average value for each value in the second dimension of the input channels. Finally, there is an output layer Fully connected layer (FC) to interconnect everything that refers to the weights of the previous output, and since we are doing a binary differentiation, we have a sigmoid activation function.

4.4.2 3D-CNN Model

The architecture for the 3D model is adjusted to the net image parameters since only the pathological and non-pathological spectrograms of both diseases were considered. In the first place, there is the first convolution layer, where important patterns for recognition, such as textures, colors, and shapes, will be selected. Mathematically this translates to filtering kernels of the same size by toning the figure with functions that model the figures of each pixel.

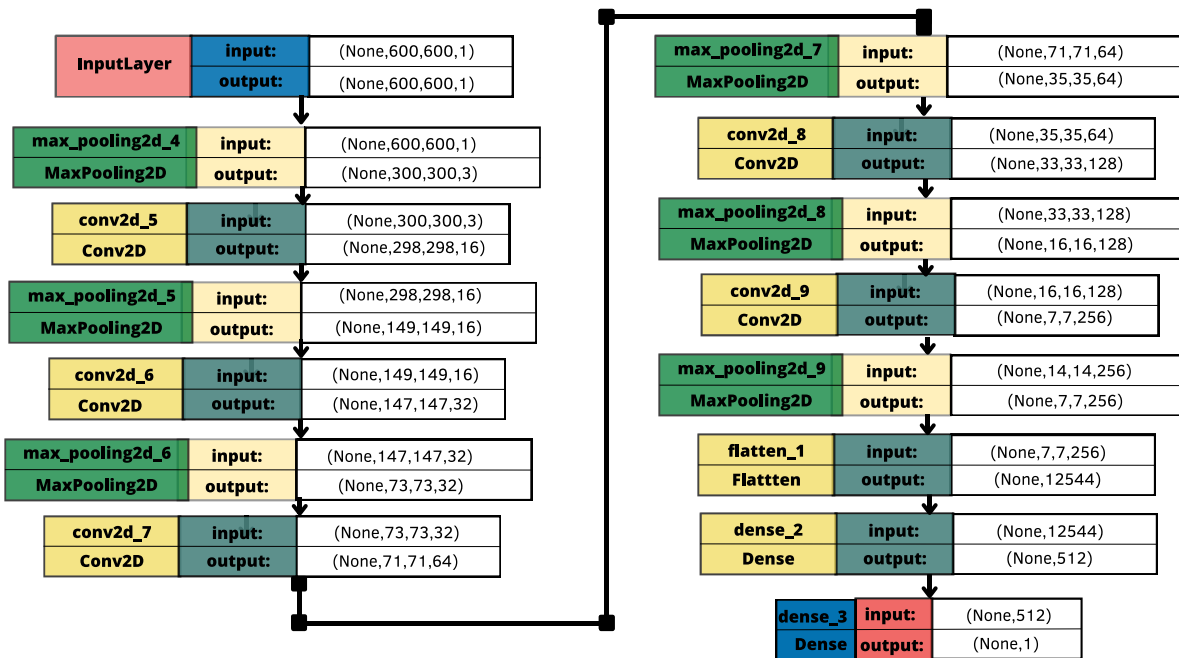


Figure 13. The architecture of the 3D prediction model is based on image classification models. Own elaboration.

The normalization batch accompanies the convolution block. This classification method performs a discretization process of the input images, but at the matrix level according to the vector arrangement of its pixels. This reduces the computational work since it reduces the size of the input matrices and, therefore, the number of parameters that the convolution layer will learn. The convolution and max pooling process is repeated in layers 5 through 9.

After the convolution, layer 9 with its respective maximum pooling. The Flatten layer will flatten the output of the previous layers by creating only one dimension from the multidimensional data without

affecting the actual size of the data batch. Finally, the output layer is found, and a dense layer contains the optimal parameters and dimensions shown in Figure 13.

4.4.3 Cross Validation

The model used the cross-validation method, which implies dividing each data (signal) into k_n parts of the same dimensions. The objective is to train as many models as parts have been divided [51].

$$(2) \quad CV_{(k)} = \sum_{k=1}^k MSE_k \frac{n_k}{n}$$

n = number of data points in total

n_k = number of data points in part k

1	2	3	4	5
T	T	T	T	V
T	T	T	V	T
T	T	V	T	T
T	V	T	T	T
V	T	T	T	T

Figure 14. Cross-validation diagram, equal segments [51].

4.4.4 L2-Regularization

A fundamental part that contributed to the excellent training and prediction of the model was the regularization methods that were applied, such as the L2 regularization method that improves the prediction errors by reducing the size of the regression coefficients, restricting them to those with the largest size to avoid overfitting [52]. The regularization function L2 contains a term that represents a bound that will not allow the convergence of the estimate until the coefficients are insignificant. It was implemented as an additional term in the loss function [53].

$$(2) \quad l = (CE(\hat{y}, y) + \alpha \frac{1}{2} \|W\|)$$

l = loss function

W = weights of the network

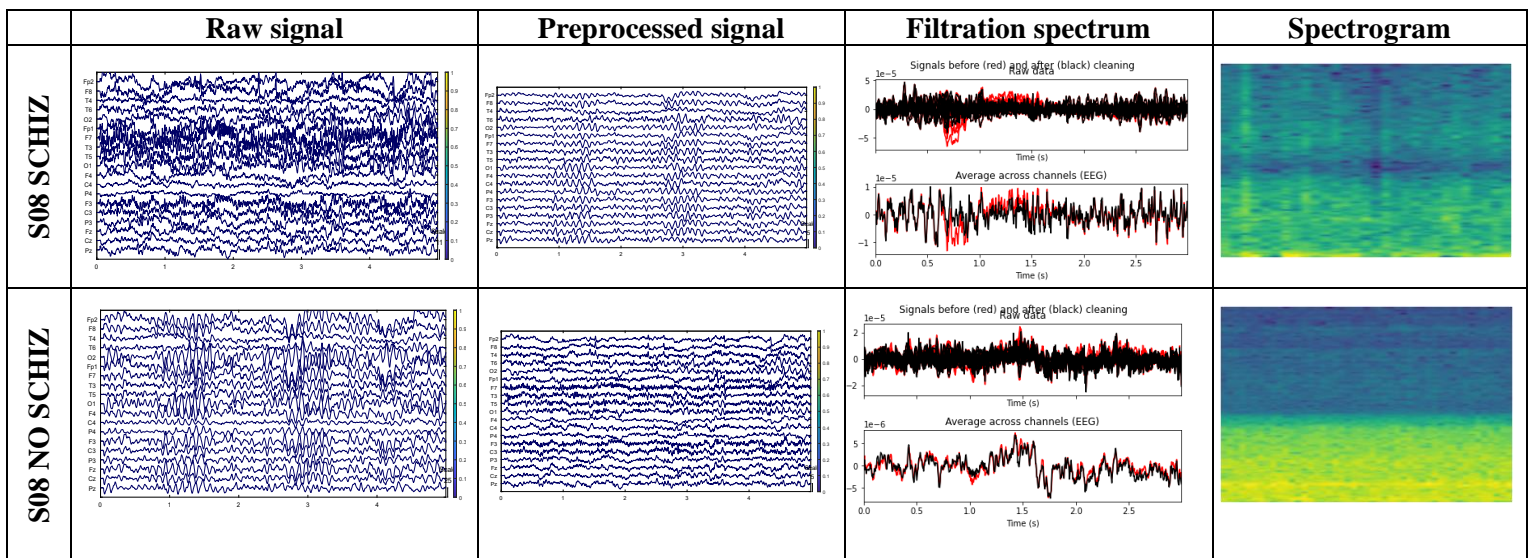
α = data points in part k

Chapter 5

Results

5.1 Signal preprocessing

The results of the processing and transformation of signals to surface images are shown in Figure 15, where raw pathological and non-pathological signals are found. That is, without processing of any kind. In the second block is the filtration and analysis of independent components of preprocessing are addressed in section 3. Third, we have the final noise filtering range compared to the initial noise of the signal. Finally, the respective spectrogram transformation for each image is shown.



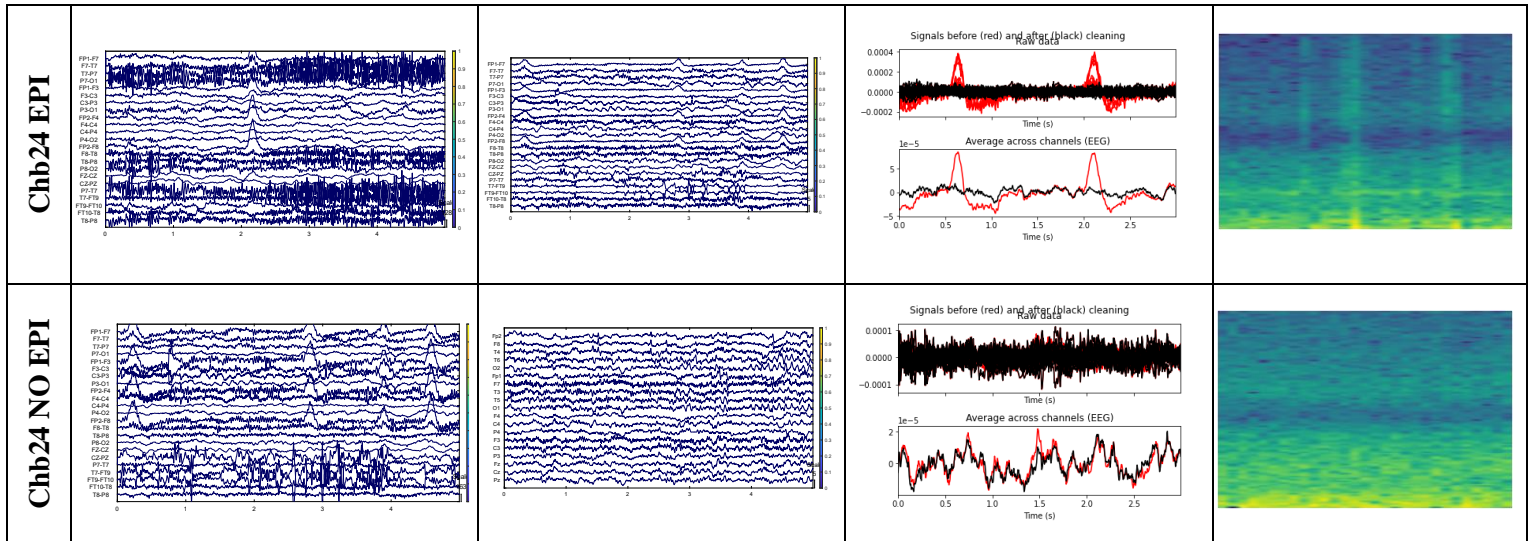


Figure 15. Preprocessing result. Data with noise and interference, data with the noise removal process, approximation of the amount of noise removed, final image spectrogram, and transformation of dimensions in data. Own elaboration.

5.2 Neural network models

5.2.1 Plots of Learning

The graphs shown in image x are the results of the 1D, and 3D neural network models, which were evaluated with respect to two important metrics that are the validation of learned data and the loss (error) of learned data. The certainty values resemble optimal prediction models. In addition, the characteristics and hyperparameters of each model are varied to optimize the predictions and reduce the error value.

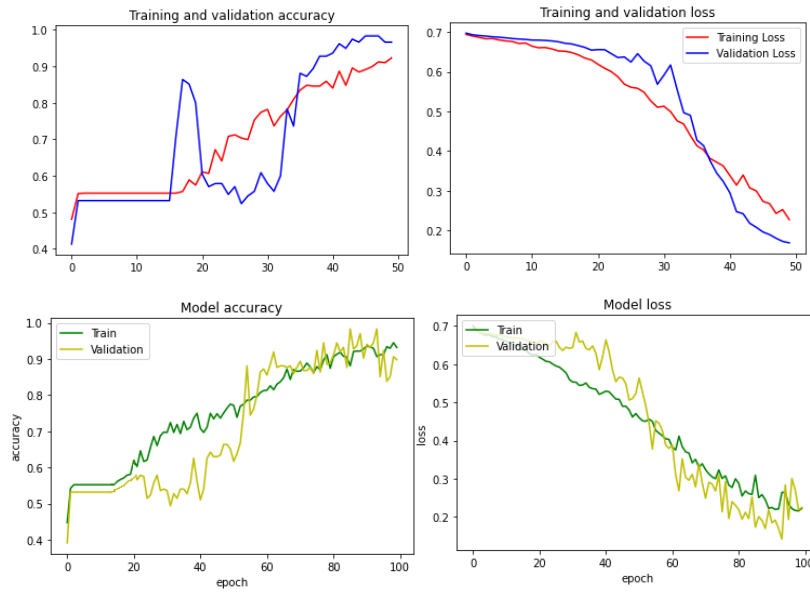


Figure 16. 1D neural model learning graphs. In the upper part, the validation by learning is shown, as well as the loss of function due to Schizophrenia with signs. At the bottom are the learning and loss function graphs for epilepsy with signs. Own elaboration extracted from GOOGLE-COLAB

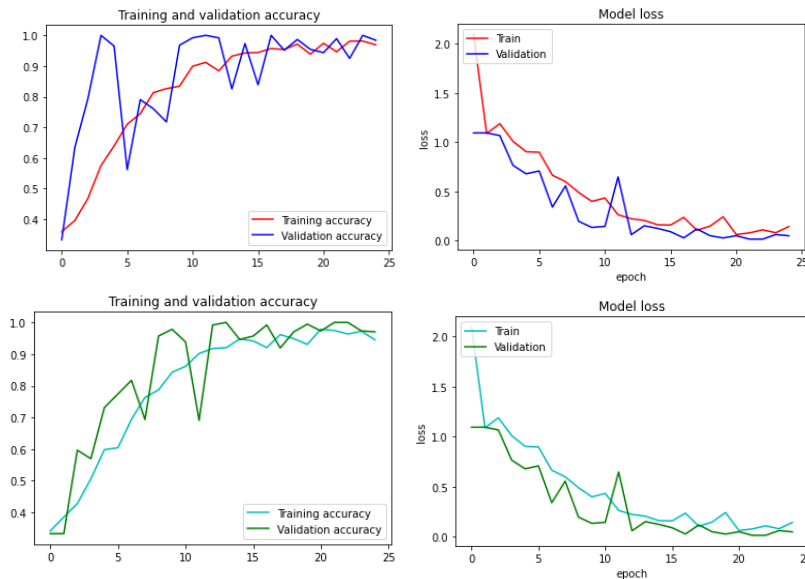


Figure 17. 3D neural model learning graphs. In the upper part, the validation by learning is shown, as well as the loss of function due to Schizophrenia with sEEGs. At the bottom are the learning and loss function graphs for epilepsy with sEEGs. Own elaboration extracted from GOOGLE-COLAB

5.2.2 Evaluation metrics

Neural network models for both 1D and 3D were successfully executed. On the one hand, with the 1D model for analyzing schizophrenic and epileptic pathologies, results shown in Table 4 were found, with a training Accuracy (Acc) of 95.0% and 89.4%, respectively, observed. On the other hand, for the analysis of surface images in schizophrenia and epilepsy, results of 96% and 95%, respectively, are shown. Other analyzes of evaluation metrics were also carried out for the factors analysis in the network that is detailed below.

Acc is the ratio between the correctly classified samples to the total number of samples. Precision is the proportion of positive samples that were correctly classified to the total number of positive predicted samples. Sensitivity represents the positive correctly classified samples to the total number of positive samples. Specificity is the ratio of the correctly classified negative samples to the total number of negative samples. The obtained values for each parameter are shown in Table 4.

$$(3) \quad ACC = \frac{TP + TN}{TP + TN + FP + FN} \quad (4) \quad PPV = \frac{TP}{TP + FP}$$

$$(5) \quad TP = \frac{TP}{TP + FN} \quad (6) \quad TNR = \frac{TN}{TN + FP}$$

Table 4. Results metrics for model performance evaluation.

	Acc	True Positive (TP)	False Positive (FP)	True Negative (TN)	False Negative (FN)	Sensitivity (TPR)	Specificity (TNR)	Precision
SZD sings	0.9500	117	0	110	8	0.9360	0.9322	1
Epilepsy sings	0.8928	211	12	89	24	0.8978	0.8811	0.9461
SZD images	0.9619	309	7	96	9	0.9716	0.9320	0.9778
Epilepsy images	0.9521	299	13	119	8	0.9739	0.9015	0.9583

Own elaboration

Chapter 6

Discussion

6.1 Data preprocessing analysis

The previous chapter takes the standard normative reference for preprocessing electroencephalographic signals. The results in chapter 5 regarding signal preprocessing indicate improvement in noise reduction, elimination of defective channels, signal resizing, and improvement in the signal transformation process. The preprocessing process in the current work guarantees a good approximation when performing the prediction stages, both in training and validation.

A fundamental aspect of carrying out the discussion is the segmentation suffered by the signals in 5-second windows. Since it allows us to obtain a more significant number of windows and eliminate punctual artifacts. The results in Figure 15 show the different stages of the input data. In the first section, the images of patient S03 without filtration are observed, representing a patient with schizophrenic events. However, overshoot channels are observed. Infiltrations are attributed to eye movement and cardiac variation. They also show non-pathological S03, epileptic chb24, and non-epileptic chb24 patients.

In the second stage, data is shown with signal cleaning stages; the main observations in this stage are the unique channeling of the signal without overlapping, in addition to eliminating a defective channel, in this case, the FT8. In the third stage, the difference in noise between without preprocessing and

preprocessed is observed. Finally, generating the spectrograms after preprocessing was important since convolution layers, and pattern stop filters in 3d models are more sensitive to noise in surface images.

6.2 Comparative analysis with other studies

Regarding the 1D model for the detection of schizophrenia (*). A comparison is made, shown in Table 5. This model is compared with the previous works on classification of EEG signals of schizophrenia patients and healthy controls in Table 3. The total Acc of 95.00% in the present work, compared to other pure convolutional models, as the ones presented by Shoebi [45] and it also performed better than traditional ML methods: KNN, Decision Trees, Naive Bayes, Random Forest, Extremely Randomized Trees and Bagging.

Table 5. Summary of recent models to diagnose schizophrenia using the czyk schizophrenia dataset.

Acc	Sensitivity	Specificity	Precision	Reference
0.9500	0.9360	0.9322	1	*
0.7143	1.0000	0.6000	0.9160	[54]
0.9300	0.9400	0.9831	0.9271	[55]
0.9071	0.9000	0.9143	0.9132	[18]
0.8453	0.7193	0.7550	-	[56]
0.9026	0.8864	0.8917	-	[57]
0.7083	0.9886	-	0.5812	[23]
0.3842	1.0000	-	0.3842	[23]
0.5685	0.9954	-	0.4724	[23]

Own elaboration

The second comparative analysis is shown in Table 6. Several schizophrenic crisis prediction models were taken with data from more than one dimension. Thus, it was compared with neural network models generated mainly with magnetic resonance image data to make comparisons of data with the exact

dimensions since it was not found with spectrogram models. A vital aspect analyzed in [59] is the reduction of the convolution layers to optimize the computational work. The point that has been subjected to several observations when we talk about neural networks is due to a long time of processing and classifying images, resulting in money when acquiring greater storage capacity and greater capacity of processors and graphics cards. On the other hand, an important observation is added: the models must be compared with other models with similar characteristics in terms of dimensions and network architecture.

Table 6. Summary of similar 3D schizophrenia prediction models.

Acc	Sensitivity	Specificity	Precision	Reference
0.9619	0.9716	0.9320	0.9778	*
0.9333	0.9489	0.9107	0.9440	[58]
0.9334	0.9460	0.9149	0.9440	[58]
0.9309	0.9394	0.9182	0.9420	[58]
0.9336	0.9425	0.9203	0.9466	[58]
0.8400	0.7300	0.8900	-	[59]
0.766	0.585	0.849	0.619	[60]
0.712	0.441	0.823	0.786	[61]
0.600	0.530	0.629	0.767	[62]

Own elaboration

The following comparison is made for detecting epilepsy diagnostic models with signals and 1D Table 7. From these, we can observe relevance in several works carried out [63] [64] that have similar approaches to the model presented and are evaluated in time and frequency. In this way, it would be interesting to investigate these values as the vital contribution made by [63], where the extraction of time and frequency characteristics in epilepsy signals is analyzed, implementing cross-validation as in the present work.

Table 7. Summary of recent models to diagnose epilepsy with signs.

Acc	Sensitivity	Specificity	Precision	Reference
0.8928	0.8978	0.8811	0.9461	*
0.8800	0.8730	0.8670	0.8708	[63]
0.8750	0.8600	0.8000	-	[64]
0.8305	0.8030	0.8580	-	[65]
0.7730	-	-	-	[66]
0.8650	0.8864	0.9070	-	[67]
0.8880	0.8770	0.9332	0.6120	[68]
0.8500	0.843	-	-	[69]
0.8683	0.7234	-	-	[70]

Own elaboration

Finally, a comparison was made between the present epilepsy prediction model with a spectrogram, for which a list of similar processes was made with different ML models. In the works cited as [71] y [72], a similar evaluation is required with the extraction of characteristics applied to a time-frequency database to which a continuous wavelet transform was applied to make scalograms. However, the difficulty of data acquisition and the amount of noise they present is proposed as one of the negative characteristics.

Table 8. Summary of recent models to diagnose epilepsy using imagen

Acc	Sensitivity	Specificity	Precision	Reference
0.9521	0.9739	0.9015	0.9583	*
0.9058	0.919	89.2	-	[73]
0.9416	0.9900	99	-	[71]
0.9355	0.9438	93.23	-	[74]
0.9480	0.9200	90.0	0.9200	[72]
0.9350	-	-	-	[75]
0.9468	0.7821	1.000	-	[76]
0.9400	0.8430	-	-	[77]
0.8600	-	-	0.8400	[78]

Own elaboration

Chapter 7

Conclusion

In conclusion, the metrics for evaluating the prediction of brain pathologies (Epileptic events and schizophrenic disorders) have a high success rate, which refers to a successful prediction model for both diseases. On the one hand, the percentage for 1D and 3D Schizophrenia was 95.00% and 96.19%, respectively. On the other hand, the prediction percentage for Epilepsy 1D, and 3D, was 89.28% and 95.21%, respectively. It was due to several factors at each stage, such as correct data filtering, noise reduction, proper manual removal of data, and correct hyperparameter and optimizer settings in neural models. The learning plots show time-adjusted values of epochs with respect to learning percentage with training and validation values.

A sufficiently robust database was also generated with signals for time-frequency analysis and surface images to analyze features by pixel. Furthermore, a critical point in the data augmentation was the time segmentation of all 1D data. It allowed us to increase the data and randomly vary it to avoid underfitting and overfitting training. In addition, there are several portals with information on the brain and neurodegenerative diseases and brain disorders. However, this information is scarce compared to the data

needed for neural training. In this sense, it is necessary to emphasize the need to create more well-labeled databases of electroencephalographic signals with free access and research use.

Furthermore, the success of predictive interventions can be concluded through comparative analysis compared to previous works with similar characteristics, such as time-frequency analysis for 1D and pixel pattern analysis through convolutional networks through filters. In addition, the improvement points that the 1D and 3D models should present were found. They are to increase the capacity of the CPU processing unit, increase the GPU graphics processing card and reduce the number of processing layers without losing features.

Finally, it is essential to mention that the results presented in this article are based on previous research regarding detecting brain pathologies and ML. Experts have validated the databases used in detecting brain pathologies. However, verifying medical prediction results by professionals specialized in detecting brain disorders is essential before making corrective decisions for pathologies.

Bibliography

1. Intersectoral Global Action Plan on epilepsy and other neurological disorders 2022 – 2031. <https://www.who.int/publications/m/item/intersectoral-global-action-plan-on-epilepsy-and-other-neurological-disorders-2022-2031>. Accessed 24 Sep 2022
2. Anuario de Nacimientos y Defunciones |. <https://www.ecuadorencifras.gob.ec/anuario-de-nacimientos-y-defunciones/>. Accessed 24 Sep 2022
3. World Health Organization (2019) WHO | Epilepsy: a public health imperative. Who 171
4. Epilepsy: a public health imperative. <https://www.who.int/publications/i/item/epilepsy-a-public-health-imperative>. Accessed 24 Sep 2022
5. Smith RG, Betancourt L, Sun Y (2005) Molecular Endocrinology and Physiology of the Aging Central Nervous System. <https://doi.org/10.1210/er.2002-0017>
6. Liao L, Madersbacher H (2019) Neurourology: Theory and practice. *Neurorol Theory Pract* 1–583 . <https://doi.org/10.1007/978-94-017-7509-0/COVER>
7. Cantile C, Youssef S (2016) Nervous System. Jubb, Kennedy Palmer’s Pathol Domest Anim Vol 1 1:250 . <https://doi.org/10.1016/B978-0-7020-5317-7.00004-7>
8. Gandhi V (2014) Brain-Computer Interfacing for Assistive Robotics: Electroencephalograms, Recurrent Quantum Neural Networks, and User-Centric Graphical Interfaces. *Brain-Computer Interfacing Assist Robot Electroencephalograms, Recurr Quantum Neural Networks, User-Centric Graph Interfaces* 1–236 . <https://doi.org/10.1016/C2013-0-23408-5>
9. Felten DL, O’Banion MK, Maida MS, Netter FH (Frank H, Perkins JA, Machado CAG, Craig JA Netter’s atlas of neuroscience. 538
10. Nakase T, Naus CCG (2004) Gap junctions and neurological disorders of the central nervous system. *Biochim Biophys Acta - Biomembr* 1662:149–158 . <https://doi.org/10.1016/J.BBAMEM.2004.01.009>
11. Noé FM, Marchi N (2019) Central nervous system lymphatic unit, immunity, and epilepsy: Is there a link? *Epilepsia Open* 4:30–39 . <https://doi.org/10.1002/EPI4.12302>
12. Clinical Electroencephalography E-Book - U. K. Misra, J. Kalita - Google Libros. https://books.google.com.ec/books?hl=es&lr=&id=ljByDwAAQBAJ&oi=fnd&pg=PP1&dq=book+of+methods+of+electroencephalography&ots=A7tU8IOEU5&sig=e2ataqF3f_zMP7W431Aq4oYWJmU#v=onepage&q&f=false. Accessed 10 Nov 2022
13. Murashko AA, Shmukler A (2019) EEG correlates of face recognition in patients with schizophrenia spectrum disorders: A systematic review. *Clin Neurophysiol* 130:986–996 .

- <https://doi.org/10.1016/J.CLINPH.2019.03.027>
14. Agustina Garcés M, Orosco LL (2008) EEG signal processing in brain-computer interface. *Smart Wheel Brain-computer Interfaces Mob Assist Technol* 95–110 . <https://doi.org/10.1016/B978-0-12-812892-3.00005-4>
 15. Amo C, de Santiago L, Barea R, López-Dorado A, Boquete L (2017) Analysis of Gamma-Band Activity from Human EEG Using Empirical Mode Decomposition. *Sensors* 2017, Vol 17, Page 989 17:989 . <https://doi.org/10.3390/S17050989>
 16. Digitalcommons@uri D, Feltane A (2016) Time-Frequency Based Methods for Non-Stationary Signal Analysis with Application To EEG Signals. Open Access Diss. <https://doi.org/10.23860/diss-feltane-amal-2016>
 17. Siuly S, Li Y, Zhang Y (2016) EEG Signal Analysis and Classification. <https://doi.org/10.1007/978-3-319-47653-7>
 18. Ciprian C, Masychev K, Ravan M, Manimaran A, Deshmukh A (2021) Diagnosing Schizophrenia Using Effective Connectivity of Resting-State EEG Data. *Algorithms* 2021, Vol 14, Page 139 14:139 . <https://doi.org/10.3390/A14050139>
 19. Danielyan A, Nasrallah HA (2009) Neurological Disorders in Schizophrenia. *Psychiatr Clin* 32:719–757 . <https://doi.org/10.1016/J.PSC.2009.08.004>
 20. Hoffman RE, McGlashan TH (2016) Book Review: Neural Network Models of Schizophrenia. <http://dx.doi.org/10.1177/107385840100700513> 7:441–454 . <https://doi.org/10.1177/107385840100700513>
 21. Oh SL, Vicnesh J, Ciaccio EJ, Yuvaraj R, Acharya UR (2019) Deep Convolutional Neural Network Model for Automated Diagnosis of Schizophrenia Using EEG Signals. *Appl Sci* 2019, Vol 9, Page 2870 9:2870 . <https://doi.org/10.3390/APP9142870>
 22. Shalhaf A, Bagherzadeh S, Maghsoudi A (2020) Transfer learning with deep convolutional neural network for automated detection of schizophrenia from EEG signals. *Phys Eng Sci Med* 2020 434 43:1229–1239 . <https://doi.org/10.1007/S13246-020-00925-9>
 23. Shoeibi A, Sadeghi D, Moridian P, Ghassemi N, Heras J, Alizadehsani R, Khadem A, Kong Y, Nahavandi S, Zhang YD, Gorriz JM (2021) Automatic Diagnosis of Schizophrenia in EEG Signals Using CNN-LSTM Models. *Front Neuroinform* 15:58 . <https://doi.org/10.3389/FNINF.2021.777977/BIBTEX>
 24. Kiranyaz S, Ince T, Abdeljaber O, Avci O, Gabbouj M (2019) 1-D Convolutional Neural Networks for Signal Processing Applications. *ICASSP, IEEE Int Conf Acoust Speech Signal Process - Proc* 2019-May:8360–8364 . <https://doi.org/10.1109/ICASSP.2019.8682194>
 25. Srinivasan V, Eswaran C, Sriraam AN (2005) Artificial Neural Network Based Epileptic Detection Using Time-Domain and Frequency-Domain Features. *J Med Syst* 2005 296 29:647–660 . <https://doi.org/10.1007/S10916-005-6133-1>
 26. Duque-Muñoz L, Espinosa-Oviedo JJ, Castellanos-Dominguez CG (2014) Identification and

- monitoring of brain activity based on stochastic relevance analysis of short-time EEG rhythms. *Biomed Eng Online* 13:1–20 . <https://doi.org/10.1186/1475-925X-13-123/TABLES/5>
27. Nigam VP, Graupe D (2013) A neural-network-based detection of epilepsy. *Biomed Eng Online* 12:55–60 . <https://doi.org/10.1179/016164104773026534>
 28. Siuly S, Li Y, Zhang Y (2016) Electroencephalogram (EEG) and Its Background. *IEEE Trans Biomed Eng* 63:3–21 . https://doi.org/10.1007/978-3-319-47653-7_1
 29. Samiee K, Kovács P, Gabbouj M (2015) Epileptic seizure classification of EEG time-series using rational discrete short-time fourier transform. *IEEE Trans Biomed Eng* 62:541–552 . <https://doi.org/10.1109/TBME.2014.2360101>
 30. Eguiagaray JG, Egea J, Bravo-Cordero JJ, García AG (2004) Neurotransmisores, señales de calcio y comunicación neuronal. *Neurocirugia* 15:109–118 . [https://doi.org/10.1016/S1130-1473\(04\)70489-3](https://doi.org/10.1016/S1130-1473(04)70489-3)
 31. Kriegeskorte N, Golan T (2019) Neural network models and deep learning. *Curr Biol* 29:R231–R236 . <https://doi.org/10.1016/J.CUB.2019.02.034>
 32. Sudeep KS, Pal KK (2017) Preprocessing for image classification by convolutional neural networks. *2016 IEEE Int Conf Recent Trends Electron Inf Commun Technol RTEICT 2016 - Proc* 1778–1781 . <https://doi.org/10.1109/RTEICT.2016.7808140>
 33. Zhong B, Xing X, Love P, Wang X, Luo H (2019) Convolutional neural network: Deep learning-based classification of building quality problems. *Adv Eng Informatics* 40:46–57 . <https://doi.org/10.1016/J.AEI.2019.02.009>
 34. Deng L, Hinton G, Kingsbury B (2013) New types of deep neural network learning for speech recognition and related applications: An overview. *ICASSP, IEEE Int Conf Acoust Speech Signal Process - Proc* 8599–8603 . <https://doi.org/10.1109/ICASSP.2013.6639344>
 35. Choi K, Fazekas G, Sandler M, Cho K (2018) A comparison of audio signal preprocessing methods for deep neural networks on music tagging. *Eur Signal Process Conf 2018-September*:1870–1874 . <https://doi.org/10.23919/EUSIPCO.2018.8553106>
 36. Subasi A, Alkan A, Koklukaya E, Kiymik MK (2005) Wavelet neural network classification of EEG signals by using AR model with MLE preprocessing. *Neural Networks* 18:985–997 . <https://doi.org/10.1016/J.NEUNET.2005.01.006>
 37. Suquilanda-Pesántez JD, Salazar EDA, Almeida-Galárraga D, Salum G, Villalba-Meneses F, Gomezjurado MEG (2022) NIFtHool: an informatics program for identification of NifH proteins using deep neural networks. *F1000Research* 11:
 38. Niles DN, Amaguaña DA, Lojan AB, Salum GM, Villalba-Meneses G, Tirado-Espín A, Alvarado-Cando O, Noboa-Jaramillo A, Almeida-Galárraga DA (2022) COVID-19 Pulmonary Lesion Classification Using CNN Software in Chest X-ray with Quadrant Scoring Severity Parameters. In: *International Conference on Smart Technologies, Systems and Applications*. Springer, pp 370–382

39. Gualsaquí MG, Delgado AS, González LL, Vaca GF, Almeida-Galárraga DA, Salum GM, Cadena-Morejón C, Tirado-Espín A, Villalba-Meneses F (2022) Convolutional Neural Network for Imagine Movement Classification for Neurorehabilitation of Upper Extremities Using Low-Frequency EEG Signals for Spinal Cord Injury. In: International Conference on Smart Technologies, Systems and Applications. Springer, pp 272–287
40. Suquilanda-Pesántez JD, Zambonino-Soria MC, López-Ramos DE, Pineda-Molina MG, Milán NS, Muñoz MC, Villalba-Meneses GF, Almeida-Galárraga D (2020) Prediction of Parkinson’s disease severity based on gait signals using a neural network and the Fast Fourier Transform. In: XV Multidisciplinary International Congress on Science and Technology. Springer, pp 3–18
41. Aguiar-Salazar E, Villalba-Meneses F, Tirado-Espín A, Amaguaña-Marmol D, Almeida-Galárraga D (2022) Rapid Detection of Cardiac Pathologies by Neural Networks Using ECG Signals (1D) and sECG Images (3D). *Computation* 10:112
42. Caicho J, Chuya-Sumba C, Jara N, Salum GM, Tirado-Espín A, Villalba-Meneses G, Alvarado-Cando O, Cadena-Morejón C, Almeida-Galárraga DA (2022) Diabetic Retinopathy: Detection and Classification Using AlexNet, GoogleNet and ResNet50 Convolutional Neural Networks. In: International Conference on Smart Technologies, Systems and Applications. Springer, pp 259–271
43. Yanchatuña OP, Vásquez PA, Pila KO, Villalba-Meneses GF, Almeida-Galárraga D, Alvarado-Cando O, Pereira JP, Veintimilla KS (2021) Skin lesion detection and classification using convolutional neural network for deep feature extraction and support vector machine
44. Tene-Hurtado D, Almeida-Galárraga DA, Villalba-Meneses G, Alvarado-Cando O, Cadena-Morejón C, Salazar VH, Orozco-López O, Tirado-Espín A (2022) Brain tumor segmentation based on 2D U-Net using MRI multi-modalities brain images. In: International Conference on Smart Technologies, Systems and Applications. Springer, pp 345–359
45. Shoeibi A, Sadeghi D, Moridian P, Ghassemi N, Heras J, Alizadehsani R, Khadem A, Kong Y, Nahavandi S, Zhang YD, Gorriz JM (2021) Automatic Diagnosis of Schizophrenia in EEG Signals Using CNN-LSTM Models. *Front Neuroinform* 15: . <https://doi.org/10.3389/fninf.2021.777977>
46. Kiranyaz S, Ince T, Abdeljaber O, Avci O, Gabbouj M (2019) 1-D Convolutional Neural Networks for Signal Processing Applications. In: ICASSP, IEEE International Conference on Acoustics, Speech and Signal Processing - Proceedings
47. Olejarczyk E, Jernajczyk W (2017) EEG in schizophrenia. <https://doi.org/10.18150/REPOD.0107441>
48. EEG in schizophrenia - IBIB PAN - Department of Methods of Brain Imaging and Functional Research of Nervous System. <https://repop.icm.edu.pl/dataset.xhtml?persistentId=doi:10.18150/repop.0107441>. Accessed 11 Nov 2022
49. CHB-MIT Scalp EEG Database v1.0.0. <https://physionet.org/content/chbmit/1.0.0/>. Accessed 11 Nov 2022
50. Shoeb A, Edwards H, Connolly J, Bourgeois B, Ted Treves S, Gutttag J (2004) Patient-specific

- seizure onset detection. *Epilepsy Behav* 5:483–498 . <https://doi.org/10.1016/J.YEBEH.2004.05.005>
51. Stone M (2007) Cross-validation:a review 2. <https://doi.org/10.1080/02331887808801414> 9:127–139 . <https://doi.org/10.1080/02331887808801414>
 52. Cortes C, Mohri M, Rostamizadeh A (2012) L2 Regularization for Learning Kernels. *Proc 25th Conf Uncertain Artif Intell UAI 2009* 109–116 . <https://doi.org/10.48550/arxiv.1205.2653>
 53. Moore RC, Denero J L 1 AND L 2 REGULARIZATION FOR MULTICLASS HINGE LOSS MODELS
 54. Buettner R, Hirschmiller M, Schlosser K, Rossle M, Fernandes M, Timm IJ (2019) High-performance exclusion of schizophrenia using a novel machine learning method on EEG data. *2019 IEEE Int Conf E-Health Networking, Appl Serv Heal 2019*. <https://doi.org/10.1109/HEALTHCOM46333.2019.9009437>
 55. Krishnan PT, Joseph Raj AN, Balasubramanian P, Chen Y (2020) Schizophrenia detection using Multivariate Empirical Mode Decomposition and entropy measures from multichannel EEG signal. *Biocybern Biomed Eng* 40:1124–1139 . <https://doi.org/10.1016/J.BBE.2020.05.008>
 56. Kim K, Duc NT, Choi M, Lee B (2021) EEG microstate features for schizophrenia classification. *PLoS One* 16:e0251842 . <https://doi.org/10.1371/JOURNAL.PONE.0251842>
 57. Krishnaveni M, Geethalakshmi SN, Subashini P, Dhivyaprabha TT, Lakshmi S (2019) Optimized backpropagation neural network model for brain computer interface system. *5th IEEE Int Smart Cities Conf ISC2 2019* 420–425 . <https://doi.org/10.1109/ISC246665.2019.9071784>
 58. Khare SK, Bajaj V, Acharya UR (2021) SPWVD-CNN for Automated Detection of Schizophrenia Patients Using EEG Signals. *IEEE Trans Instrum Meas* 70: . <https://doi.org/10.1109/TIM.2021.3070608>
 59. Shakeri M, Lombaert H, Tripathi S, Kadoury S (2016) Deep spectral-based shape features for Alzheimer’s disease classification. *Lect Notes Comput Sci (including Subser Lect Notes Artif Intell Lect Notes Bioinformatics)* 10126 LNCS:15–24 . https://doi.org/10.1007/978-3-319-51237-2_2/COVER
 60. Matsubara T, Tashiro T, Uehara K Deep Neural Generative Model of Functional MRI Images for Psychiatric Disorder Diagnosis
 61. Singh A, Westlin C, Eisenbarth H, Losin EAR, Andrews-Hanna JR, Wager TD, Satpute AB, Barrett LF, Brooks DH, Erdogmus D (2021) Variation is the Norm: Brain State Dynamics Evoked By Emotional Video Clips. *Annu Int Conf IEEE Eng Med Biol Soc IEEE Eng Med Biol Soc Annu Int Conf 2021*:6003 . <https://doi.org/10.1109/EMBC46164.2021.9630852>
 62. Suk H II, Wee CY, Lee SW, Shen D (2016) State-space model with deep learning for functional dynamics estimation in resting-state fMRI. *Neuroimage* 129:292–307 . <https://doi.org/10.1016/J.NEUROIMAGE.2016.01.005>
 63. Yao X, Cheng Q, Zhang G-Q (2019) A Novel Independent RNN Approach to Classification of Seizures against Non-seizures. <https://doi.org/10.48550/arxiv.1903.09326>

64. Al-Bakri AF, Martinek R, Pelc M, Zygarlicki J, Kawala-Sterniuk A (2022) Implementation of a Morphological Filter for Removing Spikes from the Epileptic Brain Signals to Improve Identification Ripples. *Sensors* 2022, Vol 22, Page 7522 22:7522 . <https://doi.org/10.3390/S22197522>
65. RaviPrakash H, Korostenskaja M, Castillo EM, Lee KH, Salinas CM, Baumgartner J, Anwar SM, Spampinato C, Bagci U (2019) Deep Learning provides exceptional accuracy to ECoG-based Functional Language Mapping for epilepsy surgery. *bioRxiv* 497644 . <https://doi.org/10.1101/497644>
66. Fang Z, Leung H, Choy CS (2018) Spatial temporal GRU convnets for vision-based real time epileptic seizure detection. *Proc - Int Symp Biomed Imaging 2018-April*:1026–1029 . <https://doi.org/10.1109/ISBI.2018.8363746>
67. Gasparini S, Campolo M, Ieracitano C, Mammone N, Ferlazzo E, Sueri C, Tripodi GG, Aguglia U, Morabito FC (2018) Information Theoretic-Based Interpretation of a Deep Neural Network Approach in Diagnosing Psychogenic Non-Epileptic Seizures. *Entropy* 2018, Vol 20, Page 43 20:43 . <https://doi.org/10.3390/E20020043>
68. IoT enabled Epileptic Seizure Early Detection System using Higher Order Spectral Analysis and C4.5 Decision Tree Classifier | Request PDF. https://www.researchgate.net/publication/329736857_IoT_enabled_Epileptic_Seizure_Early_Detection_System_using_Higher_Order_Spectral_Analysis_and_C45_Decision_Tree_Classifier. Accessed 10 Nov 2022
69. Zeiler MD, Fergus R (2013) Visualizing and Understanding Convolutional Networks. *Lect Notes Comput Sci (including Subser Lect Notes Artif Intell Lect Notes Bioinformatics)* 8689 LNCS:818–833 . <https://doi.org/10.48550/arxiv.1311.2901>
70. Jana GC, Agrawal A, Pattnaik PK, Sain M (2022) DWT-EMD Feature Level Fusion Based Approach over Multi and Single Channel EEG Signals for Seizure Detection. *Diagnostics* 2022, Vol 12, Page 324 12:324 . <https://doi.org/10.3390/DIAGNOSTICS12020324>
71. Liang W, Pei H, Cai Q, Wang Y (2020) Scalp EEG epileptogenic zone recognition and localization based on long-term recurrent convolutional network. *Neurocomputing* 396:569–576 . <https://doi.org/10.1016/J.NEUCOM.2018.10.108>
72. Hussein R, Lee S, Ward R (2022) Multi-Channel Vision Transformer for Epileptic Seizure Prediction. *Biomedicines* 10: . <https://doi.org/10.3390/BIOMEDICINES10071551>
73. Park C, Choi G, Kim J, Kim S, Kim TJ, Min K, Jung KY, Chong J (2018) Epileptic seizure detection for multi-channel EEG with deep convolutional neural network. *Int Conf Electron Inf Commun ICEIC 2018* 2018-January:1–5 . <https://doi.org/10.23919/ELINFOCOM.2018.8330671>
74. Nicolaou N, Georgiou J (2012) Detection of epileptic electroencephalogram based on Permutation Entropy and Support Vector Machines. *Expert Syst Appl* 39:202–209 . <https://doi.org/10.1016/J.ESWA.2011.07.008>
75. Birjandtalab J, Baran Pouyan M, Cogan D, Nourani M, Harvey J (2017) Automated seizure

- detection using limited-channel EEG and non-linear dimension reduction. *Comput Biol Med* 82:49–58 . <https://doi.org/10.1016/J.COMPBIOMED.2017.01.011>
76. Yan B, Wang Y, Li Y, Gong Y, Guan L, Yu S (2016) An EEG signal classification method based on sparse auto-encoders and support vector machine. 2016 IEEE/CIC Int Conf Commun China, ICCCHINA 2016. <https://doi.org/10.1109/ICCCHINA.2016.7636897>
77. Karim AM, Güzel MS, Tolun MR, Kaya H, Çelebi F V (2018) A New Generalized Deep Learning Framework Combining Sparse Autoencoder and Taguchi Method for Novel Data Classification and Processing. <https://doi.org/10.1155/2018/3145947>
78. Birjandtalab J, Jarmale VN, Nourani M, Harvey J (2018) Imbalance Learning Using Neural Networks for Seizure Detection. 2018 IEEE Biomed Circuits Syst Conf BioCAS 2018 - Proc. <https://doi.org/10.1109/BIOCAS.2018.8584683>

List of abbreviations

Acc: Accuracy

ANN: Artificial Neural Networks

BN: Batch Normalization

CNN: Convolutional Neural Network

Conv: Convolutional Layers

DP: Deep Learning

DSS: Decision Support Software

EEG: Electroencephalogram

GPU: Graphics Processing Unit

H: Height Dimensions

INEC: National Institute of Statistics and Census of Ecuador

ML: Machine Learning

MSP: Ministry of Public Health

NN: Neural Networks

ReLU: Rectified Linear Unit

CNS: Central nervous system

sEEG: Surface Electroencephalogram

Spctf: Specificity

TL: Transfer Learning

WHO: World Health Organization

Annex 1: EEG signal processing code and time segmentation.

```
from google.colab import drive
drive.mount('/content/drive')
path = ("URL")
raw = mn.io.read_raw_edf(path, preload= True)
raw.crop(tmin=60, tmax=120)
filt_raw=raw.copy()
filt_raw.load_data().filter(l_freq=0.5., h_freq=250)
ica=mn.preprocessing.ICA(n_components=15, max_iter='auto', random_state=97
)
ica.fit(filt_raw)

raw.load_data()
ica.plot_sources(raw,show_scrollbars=False)
ica.plot_overlay(raw, exclude=[0.0], picks='eeg')
raw.load_data()
ica.plot_sources(raw, show_scrollbars= False)
raw.load_data()
ica.plot_sources(raw,start=0, stop=5, title='Epilepsia', show_scrollbars=F
alse)
raw.load_data()
ica.plot_sources(raw, start=5, stop=10, title='No epilepsia', show_scrollb
ars=False)
```

Annex 2: Transformation code from signals (1D) to surface images (3D)

```
# use scipy.signal spectrogram to extract raw dat
from scipy.signal import spectrogram
raw = spectrogram(a[:7500], fs=125, noverlap=1)[2]

im = specgram(a[:7500], Fs=125, noverlap=1)[3]
plt.gca().set_axis_off()
plt.subplots_adjust(top = 1, bottom = 0, right = 1, left = 0,
                    hspace = 0, wspace = 0)
plt.margins(0,0)
plt.gca().xaxis.set_major_locator(matplotlib.ticker.NullLocator())
```

```
plt.gca().yaxis.set_major_locator(matplotlib.ticker.NullLocator())
plt.savefig("image.png", bbox_inches = 'tight',
           pad_inches = 0)
f._close()
```

Annex 3: 3D convolutional model for images

```
import tensorflow as tf

from tensorflow.keras.layers import Conv1D, BatchNormalization, LeakyReLU, MaxPool1D, \
GlobalAveragePooling1D, Dense, Dropout, AveragePooling1D
from tensorflow.keras.models import Sequential
from tensorflow.keras.backend import clear_session
def cnnmodel():
    clear_session()
    model=Sequential()
    model.add(Conv1D(filters=5, kernel_size=3, strides=1, input_shape=(6250, 1
9))) #1
    model.add(BatchNormalization())
    model.add(LeakyReLU())
    model.add(MaxPool1D(pool_size=2, strides=2)) #2
    model.add(Conv1D(filters=5, kernel_size=3, strides=1)) #3
    model.add(LeakyReLU())
    model.add(MaxPool1D(pool_size=2, strides=2)) #4
    model.add(Dropout(0.5))
    model.add(Conv1D(filters=5, kernel_size=3, strides=1)) #5
    model.add(LeakyReLU())
    model.add(AveragePooling1D(pool_size=2, strides=2)) #6
    model.add(Dropout(0.5))
    model.add(Conv1D(filters=5, kernel_size=3, strides=1)) #7
    model.add(LeakyReLU())
    model.add(AveragePooling1D(pool_size=2, strides=2)) #8
    model.add(Conv1D(filters=5, kernel_size=3, strides=1)) #9
    model.add(LeakyReLU())
    model.add(GlobalAveragePooling1D()) #10
```

```
model.add(Dense(1, activation='sigmoid')) #11

model.compile('adam', loss='binary_crossentropy', metrics=['accuracy'])
return model

model=cnnmodel()
model.summary()
```

Annex 4: 3D convolutional model for images

```
def create_model():
    '''Creates a CNN with 9 convolutional layers'''
    model = tf.keras.models.Sequential([
        tf.keras.layers.Conv2D(32, (3,3), activation='relu', input_shape=(30
0, 300, 3)),
        tf.keras.layers.MaxPooling2D(2, 2),
        tf.keras.layers.Conv2D(32, (3,3), activation='relu', input_shape=(15
0, 150, 3)),
        tf.keras.layers.MaxPooling2D(2, 2),
        tf.keras.layers.Conv2D(32, (3,3), activation='relu', input_shape=(15
0, 150, 3)),
        tf.keras.layers.MaxPooling2D(2, 2),
        tf.keras.layers.Conv2D(64, (3,3), activation='relu'),
        tf.keras.layers.MaxPooling2D(2,2),
        tf.keras.layers.Conv2D(128, (3,3), activation='relu'),
        tf.keras.layers.MaxPooling2D(2,2),
        tf.keras.layers.Conv2D(128, (3,3), activation='relu'),
        tf.keras.layers.MaxPooling2D(2,2),
        tf.keras.layers.Flatten(),
        tf.keras.layers.Dense(512, activation='relu'),
        tf.keras.layers.Dense(1, activation='sigmoid')
    ])

    model.compile(loss='binary_crossentropy',
                  optimizer=RMSprop(learning_rate=1e-4),
                  metrics=['accuracy'])
```